Journal of Medicinal Chemistry Article

J. Med. Chem. **2010,** *53,* 3227–3246 **3227**
DOI: 10.1021/jm9018788

Oxetanes in Drug Discovery: Structural and Synthetic Insights

Georg Wuitschik,[†] Erick M. Carreira,*[,†] Björn Wagner,[‡] Holger Fischer,[‡] Isabelle Parrilla,[‡] Franz Schuler,[‡] Mark Rogers-Evans,*[,‡] and Klaus Müller*[,‡]

[†]*Laboratorium für Organische Chemie, ETH Hönggerberg, HCI H335, 8093 Zürich, Switzerland, and* [‡]*Pharmaceuticals Division, F. Hoffmann-La Roche AG, 4070 Basel, Switzerland*

Received December 21, 2009

An oxetane can trigger profound changes in aqueous solubility, lipophilicity, metabolic stability, and conformational preference when replacing commonly employed functionalities such as *gem*-dimethyl or carbonyl groups. The magnitude of these changes depends on the structural context. Thus, by substitution of a *gem*-dimethyl group with an oxetane, aqueous solubility may increase by a factor of 4 to more than 4000 while reducing the rate of metabolic degradation in most cases. The incorporation of an oxetane into an aliphatic chain can cause conformational changes favoring synclinal rather than antiplanar arrangements of the chain. Additionally spirocyclic oxetanes (e.g., 2-oxa-6-azaspiro[3.3]heptane) bear remarkable analogies to commonly used fragments in drug discovery, such as morpholine, and are even able to supplant the latter in its solubilizing ability. A rich chemistry of oxetan-3-one and derived Michael acceptors provide venues for the preparation of a broad variety of novel oxetanes not previously documented, thus providing the foundation for their broad use in chemistry and drug discovery.

Introduction

Physicochemical and pharmacokinetic properties of compounds are explored early in the discovery process on a routine basis, and their optimization is increasingly addressed in parallel to that of target affinity and selectivity. This multidimensional optimization strategy has led to a marked improvement of the successful transition from lead discovery to the early in vivo profiling of potential drug candidates.[1] Nevertheless, compound property optimization still remains a considerable challenge in medicinal chemistry. Small molecular entities that can be easily grafted onto molecular scaffolds and modulate compound properties in distinct and predictable ways are of high interest. We have identified oxetanes as one such unit,[2] currently undergoing a renaissance[3] in medicinal chemistry[4] and having previously been largely neglected for reasons of laborious synthetic access and concerns about chemical and metabolic instability. However, it is becoming increasingly clear that the oxetane moiety can significantly enrich the toolbox of medicinal chemistry as a very small structural unit that exerts potentially far reaching property-modulating effects. In order to explore the chemistry and properties of oxetanes, we have focused on the analogies of a 3-substituted oxetane with a *gem*-dimethyl group, a carbonyl unit, and the ubiquitous morpholine unit (Figure 1).

In this paper we detail how an oxetane alters metabolic and physicochemical properties as well as structural aspects of an underlying scaffold. These findings provide guidance to understanding the influence of an oxetane on conformational preference, lipophilicity, pK_a, and metabolic stability of their host molecule. Furthermore, we report extensions and improvements of the methodology for the preparation of and access to oxetanes, not previously described.

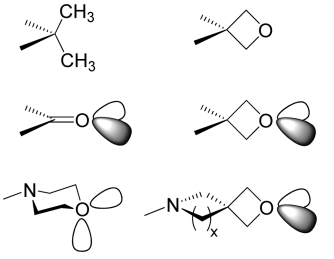

Figure 1. Oxetanes as surrogates for commonly encountered functionalities in drug discovery.

At the outset of the project we investigated oxetanes as a polar alternative to geminal dimethyl groups, which are commonly found in medicinal chemistry to introduce steric bulk, for example, embedded within tertiary butyl or isopropyl groups.[5] Commonly used to fill receptor pockets, steric bulk often also shields nearby functionalities from chemical[6] or metabolic[7] modification. Thus, in case of metabolically labile methylene groups, it is common practice to block them by the introduction of a *gem*-dimethyl unit,[8] resulting in a substantial and often undesired increase of lipophilicity. An oxetane represents a less lipophilic and metabolically more stable alternative to a *gem*-dimethyl group.

As part of many natural and synthetic feedstocks with ample methods available for their synthesis and manipulation, carbonyl compounds have become routine constituents of anthropogenic products from polymers to drugs. As a consequence of their inherent reactivity, the use of aldehydes,

*To whom correspondence should be addressed. For E.M.C.: phone, +41 44 632 2830; fax, +41 44 632 1328; e-mail, Carreira@org.chem.ethz.ch. For M.R.-E.: phone, +41 61 688 2245; fax, +41 61 688 6965; e-mail, mark.rogers-evans@roche.com. For K.M.: phone, +41 61 688 4075; fax, +41 61 688 0986; e-mail, klaus.mueller@roche.com.

Published on Web 03/29/2010

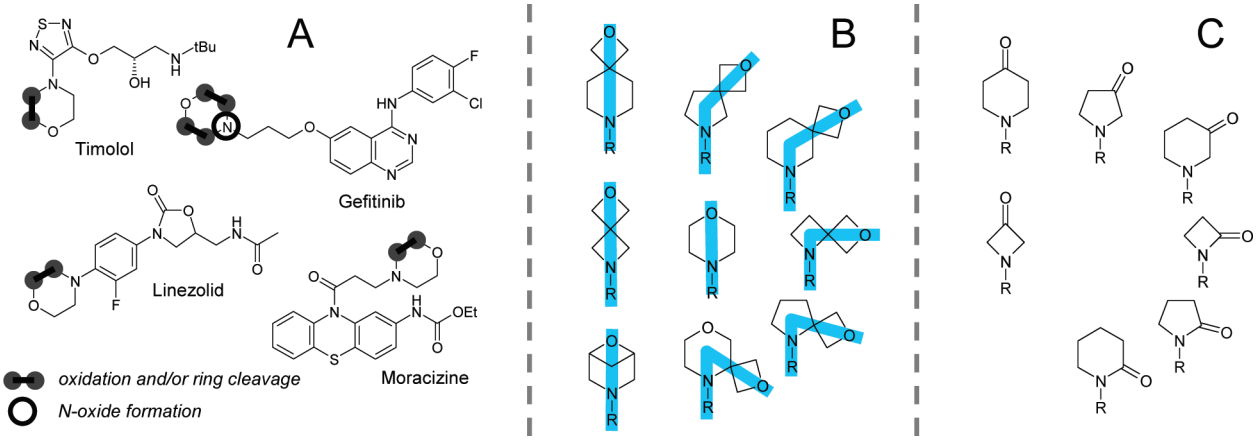

Figure 2. Marketed drugs containing a morpholine unit susceptible to metabolic oxidation (A) and spirocyclic oxetanes that could be used in place of a morpholine unit (B). The spirocyclic oxetane amines represent interesting building blocks in view of the characteristic spatial arrangement of polar surface domains (the light-blue bars mark linear or reclined arrangements of local polar units) and as possible analogues for corresponding ketoamines and lactams (C).

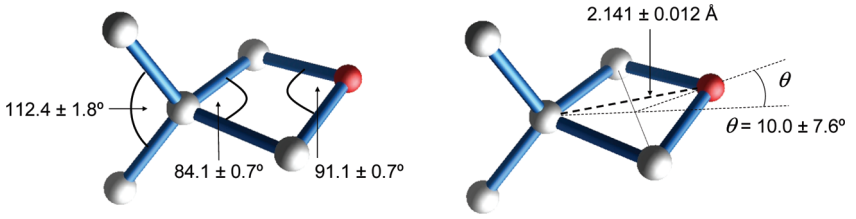

Figure 3. Averaged structural parameters obtained from nine X-ray structures of 3,3-disubstituted oxetane derivatives and two low-temperature X-ray structures of the parent oxetane, as extracted from the CSD.[11]

sterically accessible Michael acceptors,[9] or acyl halides is precluded in drug discovery. Moreover, more stable functional groups such as esters, amides, or ketones can have intrinsic liabilities associated with them in the drug discovery process. Numerous enzymes can hydrolyze esters and amides or reduce ketones. Furthermore, the relative ease of α-deprotonation in carbonyl compounds can render stereogenic centers at this position susceptible to epimerization. In such settings an oxetane unit in place of the carbonyl group, as generally depicted in Figure 1 and illustrated specifically for cyclic ketoamines or lactams in Figure 2, can provide an interesting structural alternative.

Aqueous solubility of lipophilic scaffolds is often improved by the attachment of a morpholine unit, even though morpholine is known to be a likely target of oxidative metabolism. There are 17 marketed drug substances that contain the morpholine moiety. For 13 of them metabolic data have been published,[10] and in 8 compounds oxidative degradation of the morpholine ring (Figure 2)[11] is the predominant metabolic pathway. The class of spirocyclic oxetanes shown in Figure 2 may be taken as structural analogues of morpholine in their ability to increase solubility while maintaining stability toward oxidative metabolism. However, these oxetane derivatives are intrinsically interesting building blocks through their distinct spatial distribution of polarity.

Results and Discussion

Structure and Conformation of Oxetanes. The analogies regarding 3-substituted oxetanes depicted in Figure 1 rely on limited structural knowledge[12] available from the Cambridge Structural Database (CSD).[13] Additional X-ray structures were obtained in the course of this work highlighting oxetane and its structural impact in diverse topological environments. Collectively, this set of data provides valuable insight into nonbonded interactions involving oxetanes and conformational effects induced by these small rings.

The average structural parameters for a 3,3-disubstituted oxetane are shown in Figure 3. The oxetane displays a slight widening of the exocyclic C−C−C bond angle and a small degree of puckering (measured by the dihedral angle θ). In the gas phase, microwave spectroscopy data suggest an effectively planar structure for the parent oxetane[14] with a low pucker-inversion barrier. Substitution at the 3-position leads to increased eclipsing interactions with the adjacent methylene groups, and therefore, more pronounced puckering of the oxetane ring is found in many of these structures. Nevertheless, the puckering angle remains quite small, which is important with regard to the structural analogy between an oxetane and a carbonyl unit.

An oxetane unit exerts a distinct influence on the conformational preferences of the backbone chain to which it is grafted (Figure 4). Whereas antiperiplanar conformations are favored for an unsubstituted aliphatic chain (τ = 0), all three staggered conformations are approximately equally populated at the site of a *gem*-dimethyl group (τ = 0°, 120°, and −120°). For a 3,3-disubstituted oxetane, the synclinal (gauche) conformations (τ = 120° and −120°) are clearly preferred over an antiperiplanar arrangement of the chain. This is likely a result of the small oxetane C−C−C valence angle (~84°) that leads to an increase of steric repulsion in the antiplanar backbone arrangement compared to that of a *gem*-dimethyl group.[15]

The analogy of an oxetane with a *gem*-dimethyl group draws on the experimental fact that the partial molar volume of oxetane in water (61.4 cm^3/mol at 25 °C)[17] is comparable

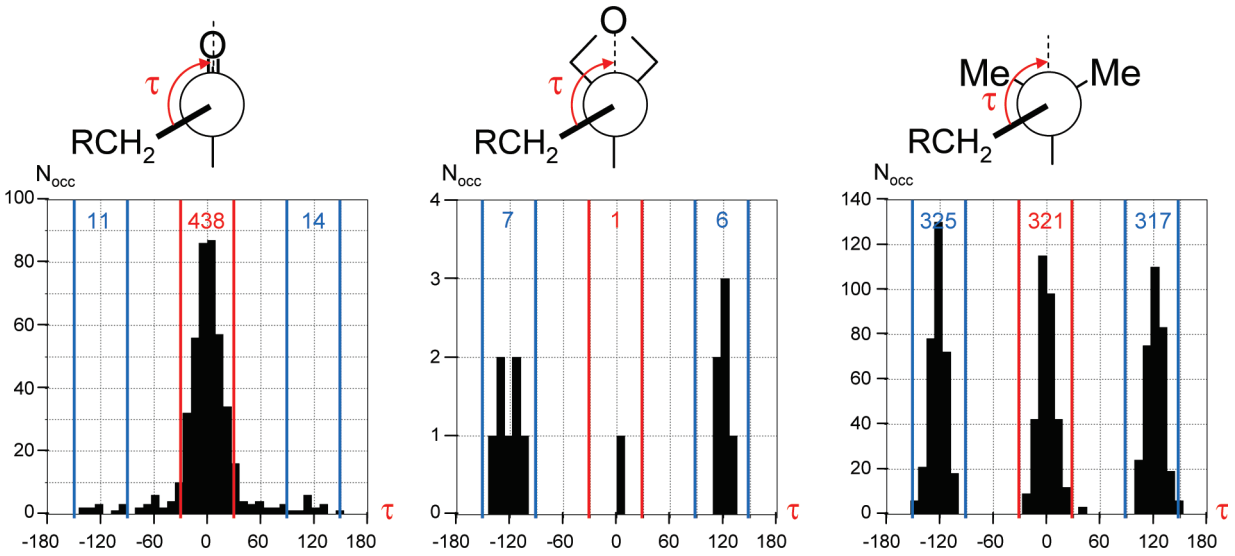

Figure 4. Arrangements of a CH_2-R group in α-position relative to an oxetane (middle), an aliphatic *gem*-dimethyl unit (right), or an aliphatic ketone carbonyl group (left), based on searches in the Cambridge Structural Database (CSD).[13,16] The torsional angle τ relates the C−CH_2 bond to the bisector of the oxetane or the *gem*-dimethyl group for better comparison with the carbonyl case. The regions of $\tau = 0 \pm 30°$ (marked in red) correspond to antiperiplanar CH_2−C−C−C backbone arrangements, whereas the regions of $\tau = \pm 120 \pm 30°$ (marked in blue) represent gauche-type backbone conformations. The red and blue numbers denote the occurrences for each τ-range.

to and even slightly smaller than that of propane (75 cm^3/mol at 25 °C).[18] Hence, bridging the two methyl groups of a *gem*-dimethyl unit by an ether oxygen introduces local and global polarity to a molecule while not increasing the partial molar volume. For the carbonyl analogy, which is based on the formal resemblance of the oxetane with the van't Hoff picture of a C=O double bond, the effects are reversed. The molar volume of an oxetane is considerably larger than that of formaldehyde,[19] since the oxygen atom is now held by two methylene groups. This increases lateral bulk and lipophilicity significantly in comparison to a carbonyl group. Furthermore, the nonbonded $C_3\cdots O$ distance in oxetane is about 0.9 Å larger than a typical C=O bond length. However, the spatial disposition of the oxygen lone pairs in a 3,3-disubstituted oxetane is similar to that of a corresponding carbonyl group (Figure 1, middle). The conformational preferences of substituents attached to a C=O double bond or to an oxetane are compared in Figure 4. Interestingly, although gauche conformations are encountered in an aliphatic backbone flanking a carbonyl group, the predominant arrangement is antiperiplanar with an aliphatic chain adopting an in-plane syn arrangement with the carbonyl group, contrasting the predominant gauche arrangement in the case of an oxetane unit.

These aspects emphasize the necessity of giving careful attention to conformational aspects when replacing *gem*-dimethyl or carbonyl groups by an oxetane unit, particularly in acyclic systems. Furthermore, for a π-conjugated carbonyl group, such as in amides, esters, lactams, or lactones, substitution by an oxetane results in a conjugative uncoupling with potential conformational rearrangement.

Structure−Property Relationships in Oxetanes. The incorporation of an oxetane not only may change the conformational preference of the underlying scaffold as discussed above but also has a marked site-dependent influence on physicochemical and biochemical properties such as lipophilicity, aqueous solubility, and metabolic stability. In order to benchmark these changes, a variety of compounds were prepared as well as their proposed congeners. Initially, a

Scheme 1. Linear Scaffold for the Incorporation of an Oxetane or a *gem*-Dimethyl Unit at Various Aliphatic Locations[a]

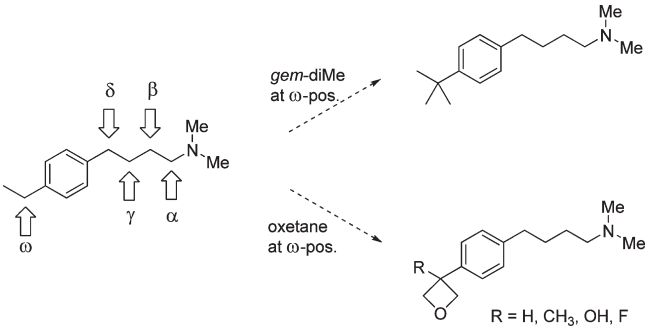

[a] Introduction of a *gem*-dimethyl group or an oxetane at the ω-position generates a *tert*-butyl group or its isosteric polar counterpart.

series of compounds was investigated in which the oxetane moiety was incorporated at different positions of the linear scaffold shown in Scheme 1.

Many of the problems encountered in drug discovery accumulate in this scaffold. It is highly lipophilic, is poorly soluble, and features different positions for metabolic attack.[20] Furthermore, the combination of a terminal basic amine and the lipophilic arylated chain renders the molecule amphiphilic and a potential candidate for causing phospholipidosis[21] and hERG channel interference.[22] This scaffold was selected in order to explore the potential benefits resulting from the incorporation of an oxetane unit.

The series of spirocyclic oxetanes (see Figure 2 and Table 1) was chosen primarily in an attempt to explore the influences of an oxetane unit in better defined conformational contexts. A comparison of the oxetanes with the corresponding carbonyl and *gem*-dimethyl substituted compounds would allow an assessment of the scope and limitation of the analogies between an oxetane and a carbonyl or a *gem*-dimethyl group. Additionally, these spirocyclic oxetanes represent novel building blocks related to morpholine **33**, and their physicochemical and biochemical properties are therefore of relevance

Table 1. Compilation of Measured Physicochemical and Biochemical Properties[h]

compound		No	log*D*[a] (log*P*)[b]	sol [c]	CL_{int} (h/m) [d]	pK_a [e]
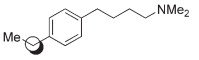	*gem*-Me_2	**1**	2.5 (5.0)	< 4	16 / 420	9.9
	oxetane	**2**	0.8 (3.3)	18,000	0 / 43	9.9
	CH_2	**37**	1.8 (4.3)	250	37 / 520	9.9
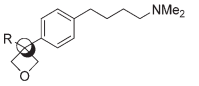	R = OH	**38**	*n.d.* [g]	300,000	0 / 68	9.6
	R = F	**39**	-0.5 (2.0)	24,000	6 / 50	9.9
	R = H	**40**	-0.1 (2.4)	17,000	2 / 27	9.9
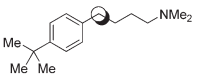	*gem*-Me_2	**3**	*n.d.* [g]	< 4	13 / 500	9.8
	oxetane	**4**	1.7 (3.9)	980	0 / 150	9.6
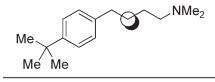	*gem*-Me_2	**5**	*n.d.* [g]	*n.d.* [g]	22 / 220	9.5
	oxetane	**6**	1.7 (3.5)	15,000	6 / 13	9.2
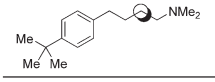	*gem*-Me_2	**7**	*n.d.* [g]	4	>1000 /	9.4
	oxetane	**8**	3.3 (4.0)	91	860 42 / 380	8.0
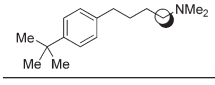	*gem*-Me_2	**9**	*n.d.* [g]	*n.d.* [g]	20 / 420	10.4
	oxetane	**10**	3.3 (3.6)	210	13 / 580	7.2
	*gem*-Me_2	**11**	0.1 (2.8)	1,700	7 / 14	10.1
	oxetane	**12**	1.3 (1.3)	6,000	21/ 26	6.2
	carbonyl	**13**	1.1 (1.1)	10,000	5 / 190	-
	*gem*-Me_2	**14**	0.8 (3.1)	1,300	0 / 16	9.6
	oxetane	**15**	0.5 (1.2)	100,000	3 / 7	8.0
	carbonyl	**16**	*n.d.* [f]	*n.d.* [f]	*n.d.* [f]	*n.d.* [f]
	*gem*-Me_2	**17**	0.9 (3.5)	180	0 /13	10.0
	oxetane	**18**	1.9 (1.9)	8,500	31 / 74	6.3
	carbonyl	**19**	1.2 (1.2)	6,800	5 / 16	-
	*gem*-Me_2	**20**	1.4 (3.7)	170	10 / 39	9.7
	oxetane	**21**	0.7 (1.5)	3,000	2 / 27	8.1
	carbonyl	**22**	-0.1 (-0.1)	19,000	100 / 580	6.1
	*gem*-Me_2	**23**	1.1 (3.9)	120	0 / 18	10.2
	oxetane	**24**	2.2 (2.4)	2,900	19 / 230	7.0
	carbonyl	**25**	1.6 (1.6)	27,000	8 / 39	-
	*gem*-Me_2	**26**	2.3 (4.3)	53	31 / 89	9.4
	oxetane	**27**	1.7 (2.3)	7,700	16 / 55	7.9
	carbonyl	**28**	0.1 (0.5)	9,000	120 / 120	7.6
	*gem*-Me_2	**29**	2.3 (4.4)	890	23 / 31	9.5
	oxetane	**30**	1.0 (2.0)	5,400	6 / 22	8.3
	carbonyl	**31**	1.2 (1.6)	17,000	120 / 88	7.5
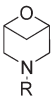		**32**	1.6 (1.8)	>11,000	15 / 41	7.1
		**33**	1.5 (1.6)	36,000	9 / 8	7.0
	x = 3	**34**	0.9 (3.1)	2,100	8 / 18	9.6
	x = 2	**35**	0.2 (2.5)	2,800	6 / 18	9.7
	x = 1	**36**	-0.1 (2.1)	13,000	0 / 11	9.5

[a] Logarithm of the *n*-octanol/water distribution coefficient at pH 7.4. [b] Intrinsic lipophilicity of the neutral base, according to $\log P = \log D + \log_{10}(1 + 10^{(pK_a - pH)})$. [c] Intrinsic molar solubility (μmol/L) of the neutral base, obtained from the experimental thermodynamic solubility in 50 mM phosphate buffer at pH 9.9 and 22.5 ± 1 °C, corrected for pK_a and rounded to 2 significant digits. [d] Pseudo-first-order rate constants, in $min^{-1}/(mg/\mu L)_{protein}$, of intrinsic clearance, measured in human (h) and mouse (m) liver microsomes. [e] Amine basicity in H_2O measured spectrophotometrically at 24 °C. For details, see Supporting Information. [f] Data not determined because of insufficient stability of compound **16**. [g] Not determined because of insufficient UV absorption. [h] R = piperonyl.

in medicinal chemistry. The *N*-piperonyl group was introduced in order to facilitate analytic measurements via UV absorption at a convenient wavelength.

Influence of Oxetanes on pK_a. The polar nature of the oxetane can be used to modulate the basicity of a proximal amine. The decrease in pK_a depends on the topological

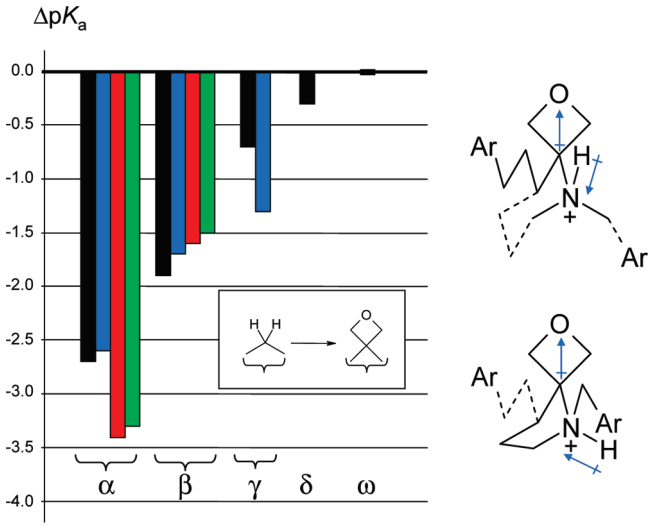

Figure 5. Change in amine basicity (ΔpK_a) by introducing an oxetane unit at different topological distances to an amine group in both acyclic (black bars) and cyclic amines (blue, red, green bars for, respectively, piperidine, pyrrolidine, and azetidine derivatives), from appropriate differences of pK_a values in Table 1. The diagram in the upper right illustrates the structural analogy of the acyclic α-case (**10**, black bar in the α-group) and the piperidine α-case (**24**, blue bar in the α-group) with an axial *N*-piperonyl substituent (see text). The diagram in the lower right illustrates the structural difference of the α-case (**10**, black bar) and the pyrrolidine α-case with a pseudoequatorial *N*-piperonyl substituent (**18**, red bar in the α-group).

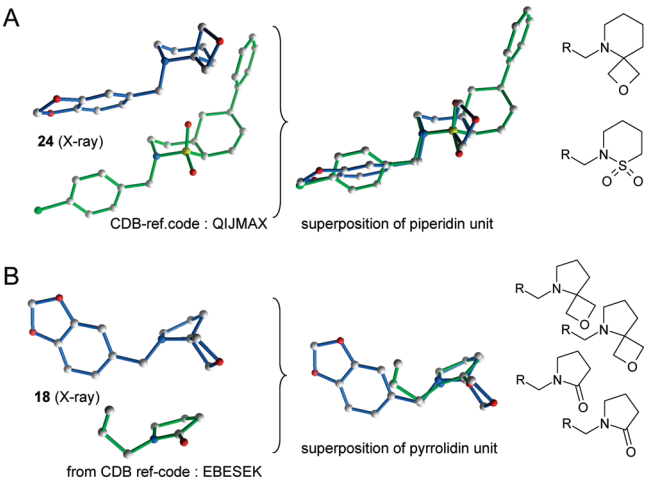

Figure 6. (A) X-ray structure of the piperidine derivative **24** with axial orientation of the piperonyl substituent, juxtaposed and superimposed with an X-ray structure of a six-membered *N*-benzyl-substituted sultam derivative (CSD reference code QIJMAX[26]) illustrating the remarkable structural relationships between these two molecular systems. (B) X-ray structure of the pyrrolidine derivative **18** with pseudoequatorial orientation of the piperonyl substituent, juxtaposed and superimposed with an X-ray structure of a five-membered *N*-alkyllactam (CSD reference code EBESEK;[27] the N-substituent was truncated after the C_γ atom for better visibility), illustrating the structural analogy between a five-membered spirocyclic α-oxetane amine and a γ-butyrolactam.

distance between the two functional units. This is illustrated in Figure 5 for various pairs of amines in which a methylene unit is replaced by an oxetane unit.

There are several aspects worth discussing in greater detail concerning the effect on amine basicity as a function of the substitution pattern. In the cyclic cases, the amine experiences the electron withdrawing effect of the oxetane via two connecting paths. One would then expect that the effect of the oxetane on the pK_a of the cyclic amines should be stronger than in the open chain case. Moreover, the effect should become more pronounced with decreasing ring size, as the topological distances between oxetane and amine become smaller for both transmission paths. This is well reflected by the piperidine derivative **24**, with the oxetane in the γ-position relative to the amine, which exhibits a pK_a shift of approximately twice that observed for the open chain γ-derivative **6** (black versus blue bars in the γ-group in Figure 5).

For an oxetane in the β-position, however, the opposite trend is found. The shifts for the cyclic systems are consistently smaller than in the open chain and decrease from piperidine to azetidine.[23] In a related study, it was found that the fluorine-induced pK_a shifts are much smaller in pyrrolidines than in piperidines. This was tentatively explained on the basis of the conformational dependence of pK_a shifts and the conformational preferences in cyclic systems. In saturated open chains and six-membered rings, well staggered conformations dominate and nonstaggered conformations become more prevalent in smaller rings, tempering through-bond transmission effects.[24] It seems likely that in the oxetane case similar effects are responsible for the decreased pK_a attenuations.

When the oxetane is located in the α-position relative to the amine, a marked decrease in basicity is found for pyrrolidine **18** and azetidine **12**. Interestingly, the pK_a decrease in the piperidine derivative **24** (−2.6) is significantly smaller than in the pyrrolidine (−3.4) or azetidine (−3.3) derivatives but quite similar to the open-chain case **10** (−2.7). As shown Figure 6, the *N*-piperonyl substituent adopts an axial position in the neutral piperidine derivative **24**, as determined by X-ray structure analysis[2b] manifesting the strong "gauche-directing" power of the oxetane unit. Thus, the piperidine derivative adopts the local arrangement about the *N*,*N*-dialkylaminooxetane that is very similar to the one in the open-chain case **10**, where N-protonation may be stabilized by antiparallel dipolar interactions. The axial position of the *N*-piperonyl substituent in protonated **24** was confirmed by detailed NMR analysis in D_2O/DCl.[2b] An X-ray structure of crystalline *N*,*N*-dimethylaminooxetane derivative **42** (see Figure 9C below) supports the suggested conformation for the acyclic case. The X-ray structure of **42** is of further interest because it illustrates not only the gauche-driving effect of the oxetane unit, placing both *N*-methyl groups synclinal to the aliphatic chain, but also the fact that antiperiplanar arrangements are tolerated when gauche conformations would imply an unfavorable (1,3)-syn-parallel arrangement (double gauche pentane) of groups, which would be inevitable when a 3-substituent at the oxetane is α-branched as in the case of **42**.

The steric congestion by the α-oxetane unit is partially alleviated in the five- and four-membered rings as a result of increased splaying of the exocyclic vicinal groups. Accordingly, for the neutral pyrrolidine derivative **18**, the X-ray crystal structure shows the *N*-piperonyl group in the equatorial position.[1] Assuming a similar arrangement also for the N-protonated form, there is then no stabilization of the protonated amine by dipolar interactions, hence the lower basicity of **18**. The same can be expected to hold for azetidine **12** (Figure 6).[25]

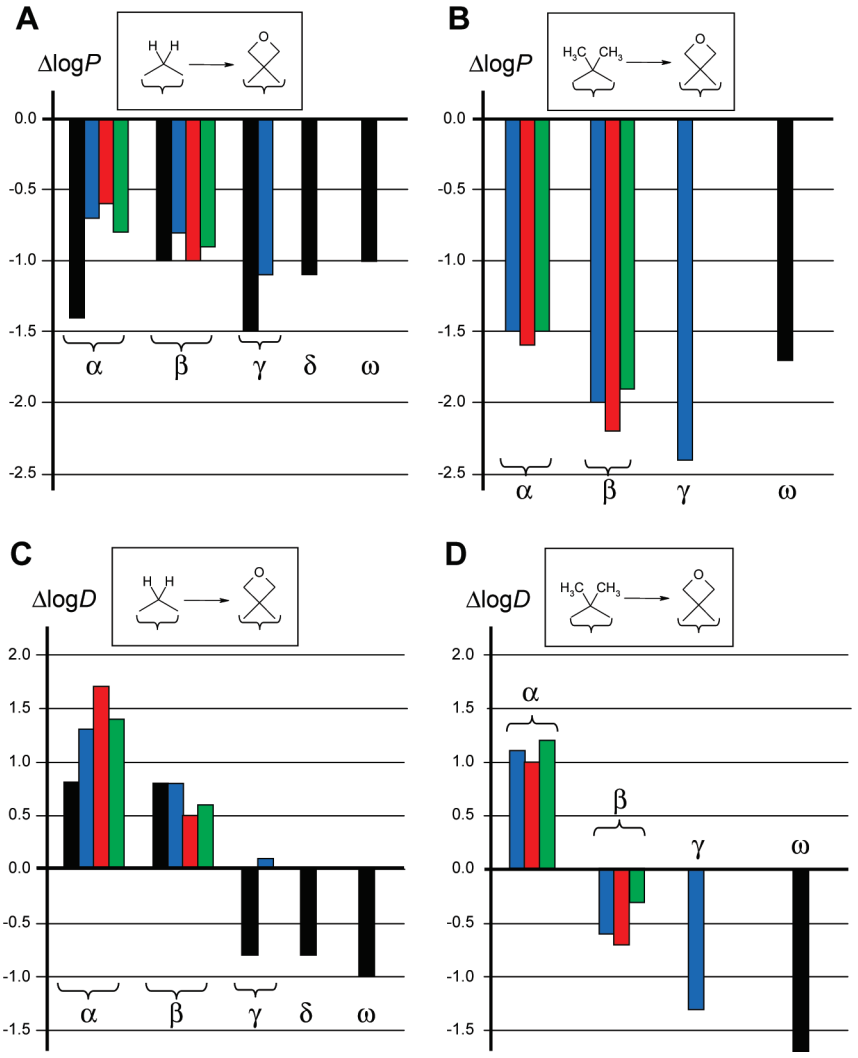

Figure 7. Change in intrinsic lipophilicity, Δlog *P*, upon exchange of a methylene (A) or a *gem*-dimethyl group (B) with an oxetane and corresponding change in lipophilicity, Δlog *D* (C, D) depending on the distance of the oxetane and the amine functionality, as obtained from corresponding log *P* and log *D* value pairs in Table 1 (black bars refer to the acyclic series; blue, red, and green bars to piperidine, pyrrolidine, and azetidine cases, respectively).

With respect to the structural analogies of these spirocyclic α-oxetaneamines with their lactam counterparts, it can be recognized that introduction of the oxetane and the absence of amide π-conjugation result in more highly puckered N-heterocyclic ring systems. However, in the pyrrolidine and azetidine cases, the γ- and β-lactams can be superimposed onto the corresponding spirocyclic α-oxetaneamine derivatives. This is illustrated in Figure 6 for the five-membered ring case (the rms deviation for the five non-hydrogen ring atoms is 0.164 Å). We note, however, that the oxetane oxygen protrudes much further from the pyrrolidine ring than the carbonyl oxygen in the butyrolactam system as discussed above. By contrast, the α-oxetane unit in the piperidine case directs the N-substituent into an axial position, much reminiscent of the situation in six-membered sultam derivatives but very distinct from δ-valerolactam derivatives (Figure 6). Indeed, superposition of the crystal structures of the spirocyclic oxetane derivative **24** and a six-membered sultam derivative[26] results in a remarkably close fit of the six non-hydrogen ring atoms (rms deviation of 0.117 Å) and a remarkably close alignment of the exocyclic pseudoaxial N−C bonds.

Influence of Oxetane on Lipophilicity. The experimental lipophilicity (log *D*) of amines, measured at pH 7.4, reflects the intrinsic lipophilicity of the neutral compound (log *P*) and the effect of (partial) protonation at the given pH. Since an oxetane unit impacts both basicity and intrinsic lipophilicity, we find it useful to separate the two effects and to assess the influence of an oxetane primarily on the intrinsic lipophilicity of the neutral scaffold.

For all molecules tested, the exchange of a methylene group by an oxetane results in a reduction of log *P* (Figure 7, upper part). Therefore, the polarity of the oxetane unit overcompensates a lipophilicity increase that may have been expected on the basis of the substantial bulk increase, similar to that of a *gem*-dimethyl group. This can be nicely seen for the triad **37**, **1**, **2** (Scheme 1 and Table 1). The transition from the *p*-ethyl to *p*-*tert*-butyl derivative (**37** → **1**) is accompanied by a lipophilicity increase of 0.7, characteristic for the introduction of two methyl groups. Introduction of the oxetane unit (**37** → **2**), however, reduces lipophilicity by 1.0 log units.

For the cyclic amine derivatives, the decrease in intrinsic lipophilicity becomes somewhat more pronounced with increasing topological separation between the oxetane and

amine. This may indicate an improved solvation of both polar functions with a larger separation of the two. However, this trend is not observed in the acyclic series, where $\Delta\log P$ effects oscillate, with polarization effects being somewhat less pronounced for an oxetane in the β- or δ-position. It is tempting to speculate on conformational effects also contributing to intrinsic lipophilicity changes. In the absence of additional structural information regarding the preferred conformations in solution, however, we refrain from a detailed interpretation of the observed effects. Moreover, the $\Delta\log P$ effects in the acyclic series may be confounded by the presence of a phenyl unit in the δ-position, which provides an entirely different structural context. Whether there will be systematic trends for intrinsic lipophilicity changes upon introduction of an oxetane into an aliphatic chain as a function of topological distance to an amine or phenyl unit remains to be seen when more compounds in the series are examined.

If the introduction of an oxetane unit does not affect the basicity of the compound, any change in the intrinsic lipophilicity, $\Delta\log P$, is directly translated to the observed lipophilicity change, $\Delta\log D$ (Figure 7, lower part). In the acyclic series, this is only the case for the oxetane introduced into the ω-position. Thus, for the five compounds **1**, **2**, **37**, **39**, and **40**, $\log P$ and $\log D$ values run in parallel (Table 1), the $\log D$ being lower by 2.5 log units than the $\log P$ because of the high degree of protonation of the amine function at pH 7.4. In going from **2** to **40**, a methyl group at the oxetane is replaced by H. The resulting decrease in lipophilicity ($\Delta\log P$ or $\Delta\log D$) of -0.9 is quite surprising in view of the typical lipophilicity change of $\sim$0.5 upon introduction of a methyl group. It may be that the H$-$C bond at the 3-position of the oxetane is strongly polarized compared to a typical aliphatic methane C$-$H unit and would be in a perfect position for π-hyperconjugative interaction with the benzene ring; these factors would then contribute to the polarity seen for compound **40**. Introduction of fluorine is generally considered to increase lipophilicity slightly.[28] However, it was pointed out recently[29] that in cases where fluorine is introduced in the β- or γ-position relative to an oxygen functionality, significant reduction in lipophilicity may be observed. The case of **39** compared to **40** ($\Delta\log P = \Delta\log D = -0.4$) appears to constitute yet another manifestation of this effect. The transition from a *tert*-butyl group to its polar 3-fluorooxetan-3-yl analogue (**1** $\rightarrow$ **39**) is particularly dramatic with a reduction in lipophilicity of 3 log units!

When introduction of an oxetane attenuates the basicity of a nearby amine function, the polarity increase is reduced in parallel with the decrease in pK_a and, hence, the degree of protonation at pH 7.4. This effect is most strongly seen in cases where the oxetane is introduced into a position α or β to the amine, but it is also noted even at topological separations as large as four single bonds between the amine and oxetane, as in compound **4**. Thus, for oxetanes located in α- or β-positions to an amine, $\Delta\log D$ effects are substantially positive, the less basic oxetane derivative being more lipophilic at pH 7.4 than its parent base. Highly consistent $\Delta\log D$ effects are observed for both the acyclic and spirocyclic series (Figure 7, lower part). For an oxetane in more remote positions (γ- or δ-position), the pK_a decrements are moderate in the acyclic cases and the polarity effects due to protonation at pH 7.4 lead to a substantial increase in polarity. By contrast, the piperidine derivative with the oxetane in the γ-position exhibits a more pronounced reduction in basicity. In this case, the pK_a lowering effectively cancels the decrease in intrinsic lipophilicity, leaving $\log D$ essentially unchanged upon replacement of a methylene group by the oxetane unit (blue bar in the γ-group in Figure 7, lower left part). This special case then constitutes what may be termed "liponeutral bulk increase".

A comparison of *gem*-dimethyl derivatives with the corresponding oxetane analogues in the spirocyclic series is quite revealing. While the same factors operate in these compounds as discussed above, the *gem*-dimethyl derivatives are more lipophilic than their parent compounds. Intrinsic lipophilicity reductions are quite dramatic, with $\Delta\log P \approx -1$ to $\Delta\log P \approx -2.5$ (Figure 7, right upper part) depending on the locus of substitution. Therefore, replacement of a *gem*-dimethyl group by an oxetane leads to an increase in lipophilicity ($\Delta\log D \approx 1$) only when this structural change is made in the α-position with its concomitant pronounced reduction of basicity, whereas for the β- and γ-positions, substantial decreases in lipohpilicity ($\Delta\log D \approx -0.5$ and $\Delta\log D \approx -1.3$, respectively) are observed (Figure 7, lower right part).

The changes in lipophilicity are reflected in the data for aqueous solubility. In order to avoid complications due to micelle formation by charged lipophilic compounds, intrinsic solubilities for the unprotonated compounds, measured at pH 9.9, are compared. For some of the more basic compounds, intrinsic solubilities were obtained from measured solubilities by appropriate pK_a corrections due to partial protonation. We caution that our reported changes of aqueous solubility have to be taken with a grain of salt because most compounds had to be measured in an amorphous and not well-defined crystalline state. However, where solubility changes are of 1 to several orders of magnitude they can probably be taken as safe trend indicators.

Figure 8 highlights the strong impact of an oxetane on the compound solubility. It is particularly marked when the underlying scaffold is highly lipophilic as in the case of the open chain scaffold (Scheme 1). Introducing an oxetane in place of a methylene group increases aqueous solubility between 25- and 4000-fold. In the more polar cyclic scaffolds the replacement of a *gem*-dimethyl group by an oxetane also leads to a pronounced improvement in aqueous solubility for all the compounds studied. The increase spans factors of approximately 4$-$4000.

For spirocyclic oxetanes, the factors leading to increase in solubility are less pronounced because the scaffolds themselves are more polar. Yet some of the oxetane derivatives show impressive gains in solubility. Remarkable in this respect is azetidine **15** with the oxetane in β-position. Its solubility of 100 000 μmol/L nears the limit of what can be reliably measured. The solubility of this compound, which we have termed "homospiro-morpholine", even surpasses the solubility of the corresponding morpholine parent **33** by a factor of 3.

To put the pronounced impact of an oxetane on lipophilicity and aqueous solubility into further context, we note that oxetanes display the most Lewis basic oxygen among cyclic ethers as documented by several experimental observations. Hydrogen-bond formation of cyclic ethers with 4-fluorophenol, studied IR-spectroscopically,[30] showed oxetane to be the strongest hydrogen bond acceptor among the cyclic ethers. Likewise, oxetane exhibits the strongest complex formation with iodine[31] and dinitrogen pentoxide.[32] In the case of iodine, a comparison of the binding constants

with oxetane and tetrahydrofuran reveals that the difference in binding strength is more pronounced than that involving hydrogen bonds. This might be a result of the higher steric demand of iodine compared to a proton, highlighting the accessibility of the electron pairs in oxetane. A study conducted on the aqueous solubility of isomeric cyclic ethers showed that compared to tetrahydropyran and 1- or 2-methyltetrahydrofuran, 3,3-dimethyloxetane was the most soluble.[33]

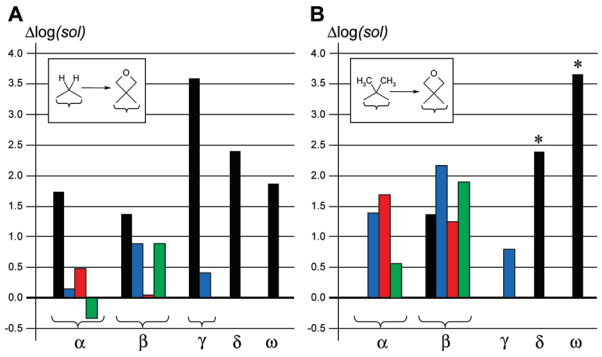

Figure 8. Logarithmic ratios by which intrinsic aqueous solubility at pH 9.9 increases upon replacement of a methylene (A) or a *gem*-dimethyl group (B) with an oxetane, as obtained from appropriate ratios of solubility value pairs in Table 1 (ratios involving the highly insoluble compounds **1** and **3** are marked by an asterisk (∗) and represent lower-limit estimates). Color codes of the bars are black for the acyclic cases and blue, red, green for the six-, five-, and four-membered cyclic amines, respectively.

The ability of an oxetane to act as a hydrogen bond acceptor and to interact in a dipolar fashion with electrophilic acceptors is also reflected in several X-ray structures. The examples shown in Figure 9 are taken from the literature and from this work; they document the accessibility of the oxetane oxygen for both Brønsted and Lewis acids. A particularly interesting example is found in the crystal structure reported by Korolev et al.[34] (Figure 9A) where the oxetane accepts a hydrogen bond from the hydroxyl group of a neighboring molecule and simultaneously engages in a dipolar interaction with the electrophilic nitrate of the neighboring molecule. A very similar hydrogen bonding interaction is seen in the crystal structure of compound **41** (Figure 9B). Each of the two crystal structures also serves to illustrate the pronounced tendency of an oxetane to stabilize gauche conformations in the backbone chain as discussed above. The crystal structure of compound **42** (Figure 9C) provides a further illustration of an orthogonal dipolar interaction of the oxetane unit with a nitro group of a neighboring molecule, the oxetane oxygen being poised on the virtual "Bürgi−Dunitz trajectory" for this group. This structure is also of particular interest in view of the stabilization of an antiperiplanar backbone chain conformation of the aliphatic 3-substituent by an α-branched substituent (*N*,*N*-dimethyl group) as discussed in the text.

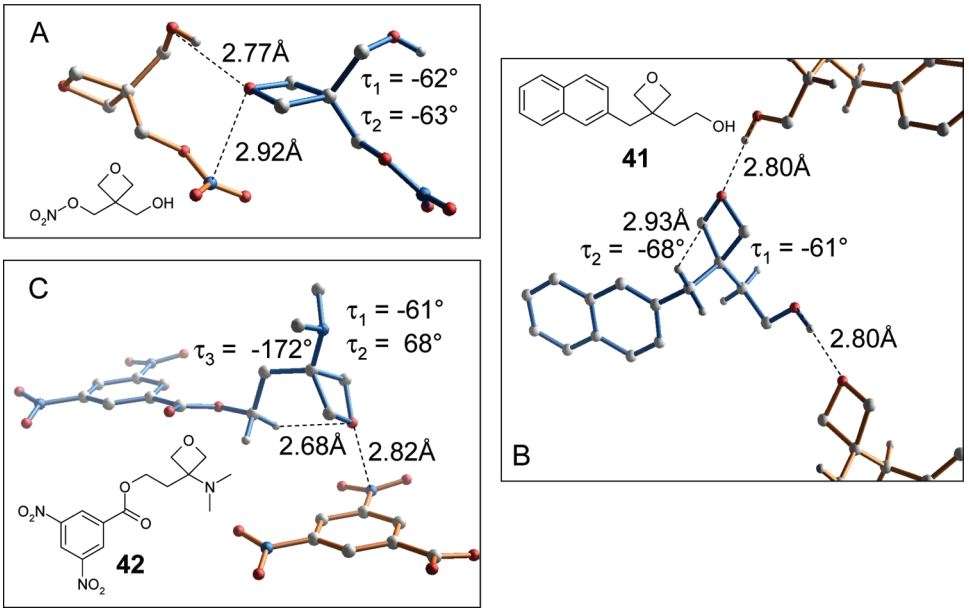

Figure 9. Examples of hydrogen bonding and dipolar interactions in oxetanes. (A) X-ray structure retrieved from the CSD (reference code IVAGUH, most H-atoms removed for better visibility[35]). The oxetane is weakly puckered ($\theta \approx 6°$), with its oxygen atom approximately positioned along the "Bürgi−Dunitz trajectory" for nucleophilic interaction with the nitrate group with angles of 78°, 93°, and 97° between the O···N vector and the nonterminal and terminal N−O bonds, respectively. The dioxypropane backbone adopts a pseudo-C_2-symmetrical gauche−gauche conformation, illustrating the marked tendency of oxetanes to stabilize gauche arrangements in the backbone chain. (B) Crystal structure of compound **41** (most H-atoms removed for better visibility) with two neighboring molecules engaging in hydrogen bonds between the oxetane and a hydroxyl group. The oxetane ring is moderately puckered ($\theta \approx 12°$), with its oxygen atom inclined toward one hydrogen atom of the benzylic methylene group. The chain backbone adopts again a pseudo-C_2-symmetrical gauche−gauche conformation at the site of the oxetane. (C) Crystal structure of compound **42** (most H-atoms removed for better visibility). The oxetane oxygen atom is situated again approximately on a "Bürgi−Dunitz trajectory" for a nucleophilic interaction with one of the two electrophilic nitro groups with angles of 75°, 96°, and 97° between the O···N vector and the N−C and the two terminal N−O bonds, respectively. The 3-ethyloxy substituent adopts an antiperiplanar backbone conformation at the oxetane (see text, $\tau_{NCCC} = -172°$) and is further twisted with a torsion angle of $\tau_{CCCO} = -160°$, bringing one methylene hydrogen atom into proximity for weak but potentially favorable electrostatic interactions with the oxetane oxygen atom. The oxetane ring is markedly puckered ($\theta \approx 17°$), bringing the O-atom into proximity of this methylene unit and at the same time avoiding an unfavorable interaction with the amine N-lone pair electrons.[36]

Comparison of the hydrogen bonding avidity of oxetane with various carbonyl compounds demonstrates that oxetanes can compete favorably with aliphatic ketones, aldehydes, or esters[27] (Figure 10), which is of interest in view of a similar spatial disposition of the oxygen lone pairs as in a carbonyl unit (Figure 1, middle). However, an oxetane is a much weaker hydrogen bond acceptor than an amide carbonyl group (Figure 11). This is important to remember, apart from structural or basicity aspects (see above), when considering the replacement of an amide or lactam by a 3-amino-oxetane unit.[38]

An oxetane analogue is typically more lipophilic than its carbonyl counterpart because of the presence of two methylene groups in the four-membered ring. The effect is most pronounced for β-ketopiperidine and β-ketopyrrolidine, which are both unusually polar, possibly as a consequence of the (1,3)-syn juxtaposition of the polar carbonyl and amine or protonated amine functions with dipolar enhancement as well as possibilities for cooperative solvation. By contrast, the amine and ether oxygen functions are insulated from each other by an intervening methylene group of the oxetane ring in the β-spirocyclic analogues, as illustrated in Figure 12.

In view of the structural analogies between the spirocyclic oxetane amines and morpholine, a direct comparison of their lipophilicities and solubilities is instructive (Figures 13 and 14). Although intrinsic lipophilicity is observed to increase in all oxetane derivatives of piperidine (**24**, **27**, **30**), the azetidine analogues (**12**, **15**) are more polar than the corresponding morpholine derivative (**33**, green bars in Figure 13), despite the fact that the spiro-oxetane derivatives of azetidine contain an extra carbon atom compared to morpholine. The pyrrolidine analogues (**18**, **21**) are intermediate with intrinsic lipophilicities quite similar to that of the morpholine derivative. For purposes of comparison we include here the (3,5)-methano-bridged morpholine analogue **32** which also exhibits very similar lipophilicity as its parent morpholine derivative.

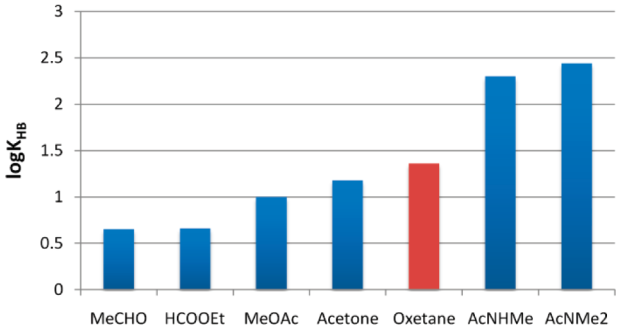

Figure 10. Hydrogen bond acceptor avidity for oxetane and different carbonyl compounds as measured by H-bonded complex formation in CCl_4.[37]

For log *D*, the basicity-reducing factor of the oxetane module adds to the pattern seen for log *P*, resulting in dramatic polarity increases for the more basic spirocyclic amines with the oxetane unit in β- or γ-position to the nitrogen. Thus, the lipophilicity (log *D*) of the β-spiro-oxetane analogue **27** is comparable to that of the morpholine derivative **33** (Figure 13 right, blue bar in β-group), whereas the γ-analogue **30** is considerably more polar. Moreover, the β-spiro-oxetanes in the pyrrolidine and azetidine series, compounds **21** and **15** (Figure 13 right, red and green bars, respectively, in the β-group), are significantly less lipophilic than the morpholine counterpart.

By virtue of its polarity, the morpholine unit often helps to improve the solubility of a compound into which it is integrated. Remarkably, the *N*-piperonylmorpholine derivative **33** has the highest solubility (36000 μmol/L) of all compounds without an oxetane in this study. When morpholine derivative **33** is compared with its spirocyclic analogues (Figure 14, right), it is found to be more than twice as soluble. This result is remarkable in view of the higher polarity of at least some of the spirocyclic oxetane amine derivatives. The "homospiro-morpholine" **15** is one notable exception (green bar in the β-group), however, as already noted above. This highlights the "homospiro-morpholine" as a very promising solubilizing unit.

In Figure 14 (left) we include a comparison of the solubilities of the spirocyclic oxetane amines with the corresponding cyclic ketoamines or lactams. It illustrates that all but one carbonyl derivative in this study are more soluble than the more lipophilic oxetane analogues. The exception is the case of the spirocyclic α-oxetanepyrrolidine derivative **18** (red bar in the α-group) that is slightly more soluble than its γ-butyrolactam counterpart **19**. Unfortunately, the azetidine-3-one **16** could not be included in this study because of its inherent instability under various analytical conditions, thus precluding a direct comparison with the highly soluble β-oxetane amine analogue **15**.

Chemical Stability. All 3,3-disubstituted oxetanes described here were found to be stable when subjected to treatment in aqueous solutions, buffered at pH 1−10, for 2 h at 37 °C

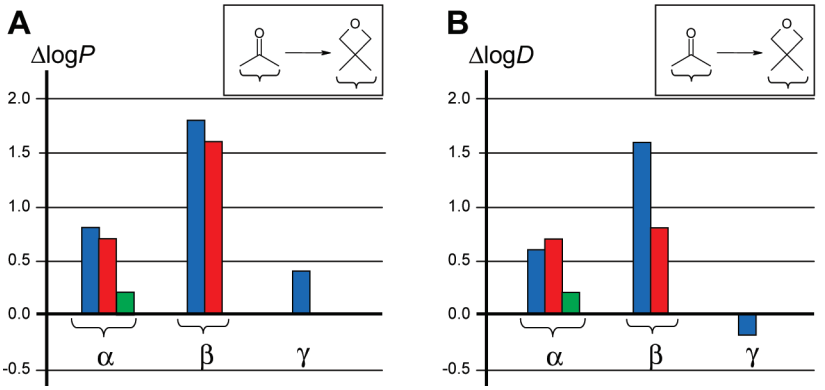

Figure 11. Changes in log *P* (A) and log *D* (B) upon replacement of a carbonyl group by an oxetane, as obtained from appropriate log *P* and log *D* value pairs in Table 1. Color codes of the bars are blue, red, and green for the six-, five-, and four-membered cyclic cases, respectively.

(for details see Supporting Information). Their stability toward acid-catalyzed ring-opening at low pH values is quite remarkable and is particularly noteworthy for the strained oxetanes **12** and **15**. The chemical stability of **15** is in striking contrast to the corresponding aminoketone analogue **16** mentioned above. For oxetane derivatives carrying only one substituent at the 3-position, some decomposition could be observed under strongly acidic conditions. Thus, oxetane **40**, while fully recoverable after corresponding treatments in the pH range of 4−10, exhibited partial decomposition at pH 1 with ∼83% recovery.

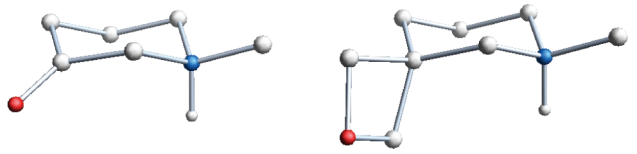

Figure 12. Juxtaposition of molecular models of N-protonated *N*-methyl-3-ketopiperidine (left) and *N*-methyl-3-oxetanopiperidine, illustrating the (1,3)-syn juxtaposition of the carbonyl unit to the polar amine or protonated amine group in contrast to the 3-oxetane derivative in which the polar ether unit is insulated from the amine or protonated amine function by a methylene group of the oxetane ring. This may explain the marked difference in lipophilicity (both log *P* and log *D*) in compound pairs **27**/**28** and by analogy **21**/**22**.

Oxetanes show remarkable stability to many reaction conditions that would compromise the integrity of epoxides. Nucleophilic opening of oxetanes requires in most cases the use of strong Lewis acids;[39] under alkaline conditions alone, oxetanes are known to open much more slowly than oxiranes.[40] Our experience confirms these findings, showing no sign of ring-opening when treating oxetanes with organometallic reagents, amines, or alkoxides.[41] The introduction of double substitution on the 3-position not only significantly reduces ring strain[42] but also reduces the susceptibility to ring cleavage via nucleophilic displacement by increasing unfavorable nonbonded interactions that are analogous to those observed at neopentyl centers. Therefore, 3,3-disubstituted oxetanes are in general more resistant to decomposition than monosubstituted ones. This is reflected in their stability toward lithium aluminum hydride which slowly opens 3-monosubstituted oxetanes already at −78 °C, whereas 3,3-disubstituted oxetanes show no reaction at 0 °C. Concentrated acid is problematic for both groups and can lead to decomposition, for example, when trying to cleave a Boc group.[41]

Metabolic Stability of Oxetanes. All the compounds tested in this study were subjected to standardized preparations of human and mouse liver microsomes, and the remaining unchanged material was determined at several time intervals during 2 h of incubation at 37 °C. This test yields

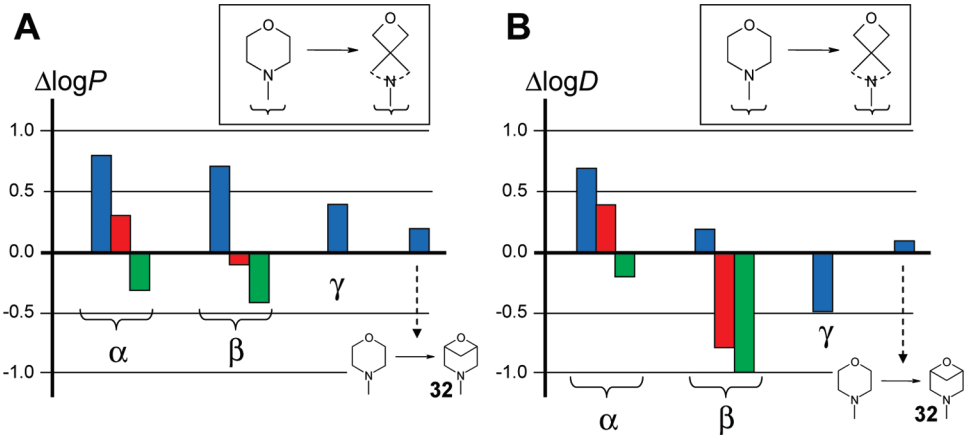

Figure 13. Changes in log *P* (A) and log *D* (B) upon replacement of the morpholine unit by the various spirocyclic analogues, including the bicyclic oxetane derivative **32**, as obtained from appropriate log *P* and log *D* value pairs in Table 1. The color codes of the bars are blue, red, and green for six-, five-, and four-membered cyclic amine systems, respectively.

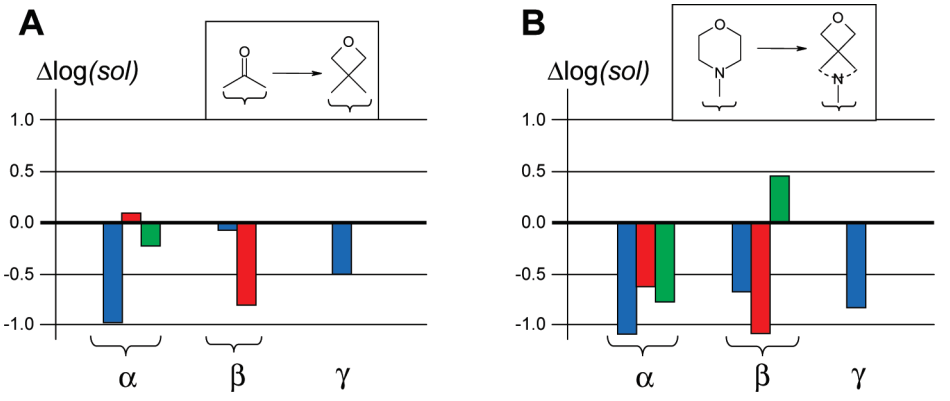

Figure 14. Logarithmic ratios by which intrinsic molar solubility at pH 9.9 changes upon replacement of a carbonyl group by an oxetane unit (A) or a morpholine by a spiro-oxetane amine moiety (B), according to solubility value pairs in Table 1. The color codes of the bars are blue, red, and green for six-, five-, and four-membered cyclic amine systems, respectively.

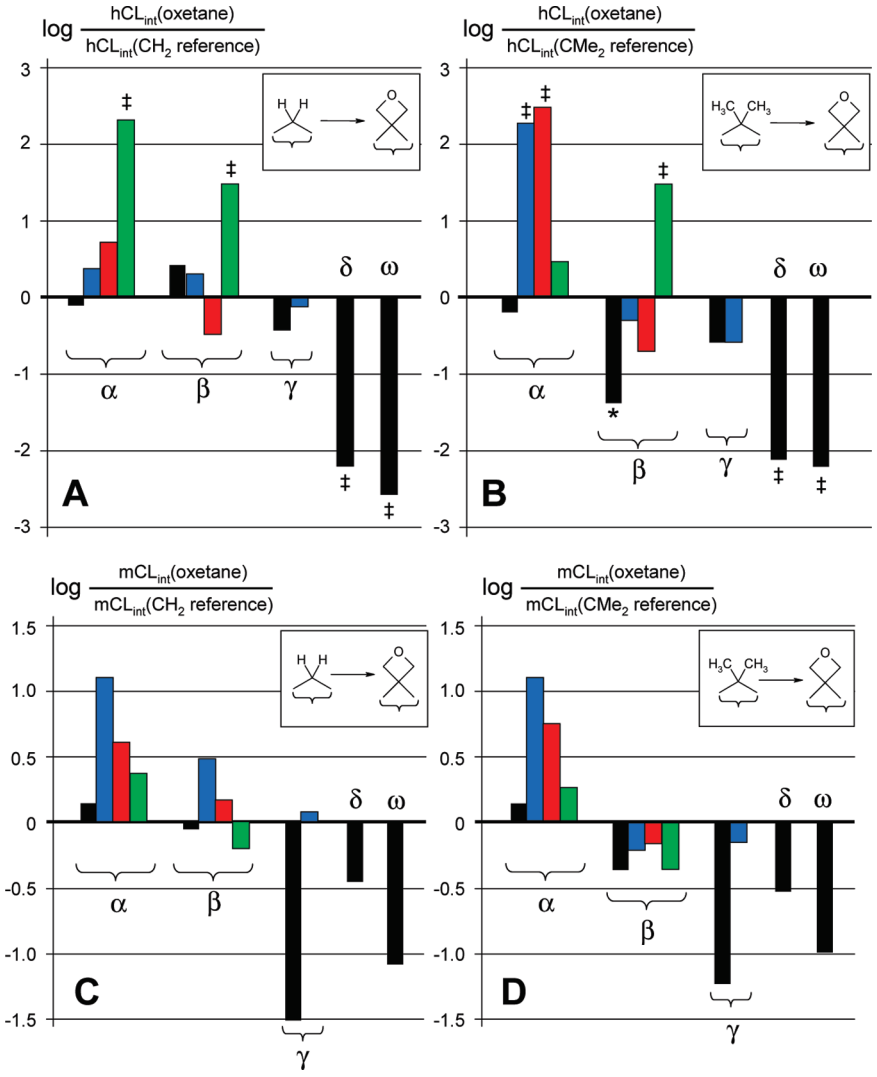

Figure 15. Logarithmic ratios of intrinsic clearance rates (CL_{int}), measured in human (A, B) and mouse (C, D) liver microsomal assays upon introduction of an oxetane at the site of a methylene group (A, C) or replacing an aliphatic *gem*-dimethyl unit (B, D), as obtained from corresponding value pairs in Table 1. Black bars refer to the acyclic series; the blue, red, and green bars relate to piperidine, pyrrolidine, and azetidine derivatives, respectively. (‡) Where $CL_{int} \approx 0$ min^{-1}/(mg protein/μL), it was replaced by the value 0.1 to avoid extreme values in ratios or their logarithm. (∗) CL_{int} for the *gem*-dimethyl reference compound **7** was set at 1000 min^{-1}/(mg protein/μL).

pseudo-first-order rate constants for oxidative degradation, intrinsic clearance rates (CL_{int}), that provide useful indications for phase I metabolism. Although metabolic susceptibility of a molecular subunit depends much on the structural context in which it is embedded as well as on the overall lipophilicity of the compound, some general patterns can be observed from the pairwise comparisons displayed in Figure 15 for human and mouse liver microsomal assays.[43] For the majority of cases, the introduction of an oxetane results in a marked reduction of metabolic susceptibility. This is evident from the ratios of intrinsic clearance rates in both human and mouse microsomal assays. Pronounced reductions in oxidative susceptibility result when a *gem*-dimethyl group is replaced by the polar oxetane unit (Figure 15B,D), while they are somewhat more moderate when the oxetane unit is introduced at the site of a methylene group (Figure 15A,C). Most prominent cases are oxetane derivatives **2** and **4** in the acyclic series, in which the introduction of an oxetane unit in either of the two benzylic positions (ω- and δ-position relative to the basic amine) results in complete silencing of oxidative degradation by human liver microsomes. Since these two cases are the only ones with an oxetane unit at such a position, it will be important to explore further the potential of blocking oxidative metabolism by placing an oxetane into a benzylic position.

Notable exceptions to the general trends are the cases in which an oxetane unit is placed in the α-position relative to a basic amine. In almost all of these cases, the clearance rates increase. We interpret this finding as resulting from the strong basicity-lowering effect on the amine by the close oxetane unit, rendering the compound much more lipophilic (log *D*) than its parent amine and thus increasing its exposure to membrane-bound cytochrome P450 enzymes. A similar, if somewhat attenuated, effect is seen for some of the compounds containing an oxetane unit in β-position relative to a basic amine. In such cases, the basicity-lowering effect remains prominent, but it is less pronounced than in those cases involving α-substitution. We also note that an increased metabolic attack is only observable for compound pairs in which an oxetane unit is introduced in place of a methylene group. Replacement of a *gem*-dimethyl group by

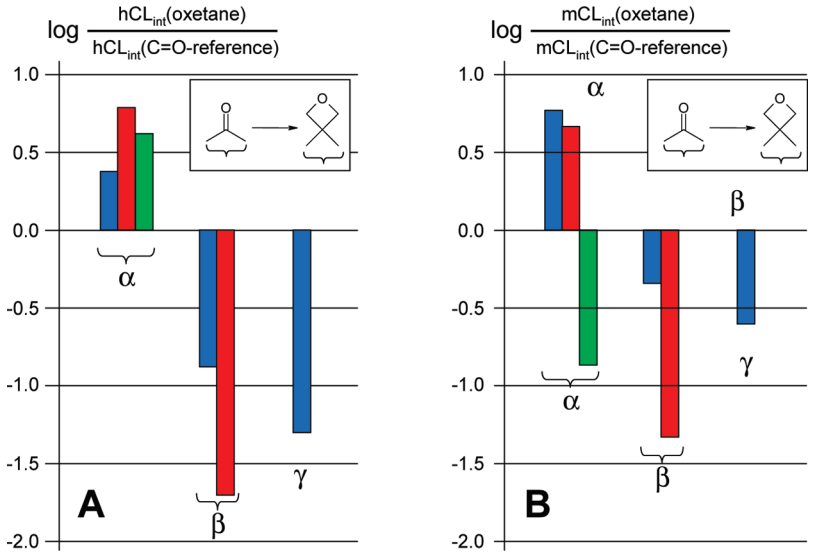

Figure 16. Logarithmic ratios of intrinsic clearance rates (CL_{int}), measured in human (A) and mouse (B) liver microsomal assays, upon introduction of an oxetane in place of a carbonyl group, as obtained from corresponding value pairs in Table 1. Bar color codes are blue, red, and green for piperidine, pyrrolidine, and azetidine derivatives, respectively.

an oxetane unit in β-position relative to an amine reduces clearance rates in essentially all cases studied, in conformity with the general trends noted above. The one seeming exception, the "homospiro-morpholine" derivative **15** in comparison to the 3,3-dimethylazetidine derivative **14** (Figure 15B, green bar in the β-substitution group), is the case where both compounds are metabolically quite stable. The dimethylated reference compound **14** is remarkably inert to oxidative metabolism as is the β-oxetane derivative **15**. The same holds true for spirocyclic oxetaneamines **12** and **15** compared to azetidine derivative **36** (Figure 15A). Although **15** is essentially inert under human assay conditions, **12** and **15** are slowly oxidized by mouse liver microsomes. However, the azetidine derivative **36** is surprisingly inert under the same conditions, possibly as a consequence of the very low lipophilicity of **36**. By contrast, both spirocyclic oxetaneazetidine derivatives **12** and **15** are more lipophilic as a consequence of substantially increased bulk and reduced amine basicity. The remarkable stability of the "homospiro-morpholine" derivative **15** in human and mouse liver microsomal assays highlights this spirocyclic amine again as a promising building block for medicinal chemistry.

The spirocyclic oxetaneamines display significantly higher metabolic stabilities than their β-keto- and γ-ketoamine counterparts (Figure 16). Indeed, while cyclic β- and γ-ketoamines **22**, **28**, and **31** are quite rapidly decomposed in the microsomal assays,[44] the corresponding spirocyclic oxetaneamines **21**, **27**, and **30** have low to only moderate clearance rates.

In this context, another comparison is of interest. Replacement of γ-piperidone **31** by its oxetane counterpart **30** will lead to an increase in the distance between the polar nitrogen and oxygen atoms by approximately 0.9 Å, but a replacement of γ-piperidone **31** by the smaller "homospiro-morpholine" **15** results in an almost perfect superposition of the nitrogen and oxygen heteroatoms (Figure 17). The spirocyclic oxetane **15** is once again identified as an interesting building block that can be used to replace a potentially labile γ-piperidone by a spatially comparable, somewhat more polar and much more soluble, metabolically more robust building block of similar moderate amine basicity.

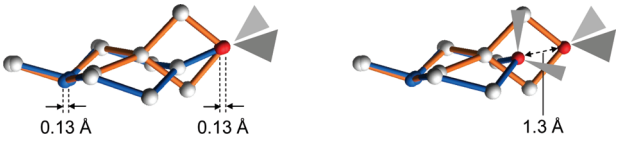

Figure 17. Rigid superpositions of an X-ray structure-derived model of *N*-methyl-"homospiro-morpholine" (orange; X-ray structure of *N*-benzhydryl-2-oxa-6-azaspiro(3.3)heptane[2b] to X-ray structure-derived models of *N*-methyl-γ-piperidone[45] (blue, left) and *N*-methylmorpholine[46] (blue, right)). An almost perfect match of the heteroatoms is achieved for the superposition on the left. The spatial disposition of the oxygen lone pairs in the morpholine, "homospiro-morpholine", and γ-piperidone units is indicated by gray wedges.

Lactams exhibit higher metabolic stability. It is interesting that even the β-lactam derivative **13** is comparatively stable in human liver microsomes. Only in the mouse microsomal assay is this lactam destroyed more rapidly. This is then the only case in which the α-spirocyclic oxetane analogue **12** compares favorably against its lactam counterpart (see Figure 16B, green bar in the α-group), while in all other cases of α-spirocyclic oxetaneamine versus lactam the former show slightly higher if still moderate clearance rates. Piperidine derivative **34** displays low to moderate clearance rates in human and mouse liver microsomes, respectively (Table 1). Likewise, morpholine derivative **33** is fairly stable in both microsomal assays. Direct comparison of the various spirocyclic oxetaneamines with piperidine derivative **34** (Figure 18 A,B) shows that introduction of an oxetane unit only moderately affects the low clearance rates. If the oxetane is placed α to the basic amine, lipophilicity increases because of basicity reduction, and a slight increase in clearance rates is observed. Introduction in the γ-position results in a reduction of the clearance rate, while a placement of the oxetane in β-position leads to a slight increase in clearance for the piperidine scaffold but improved stability for the pyrrolidine or azetidine scaffolds. The pattern is very similar in a comparison of spirocyclic amines with the morpholine derivative **33** (Figure 18 C,D) as far as human microsomal assay data are concerned. For the mouse microsomal data (Figure 18D), the logarithmic ratios of clearance rates are

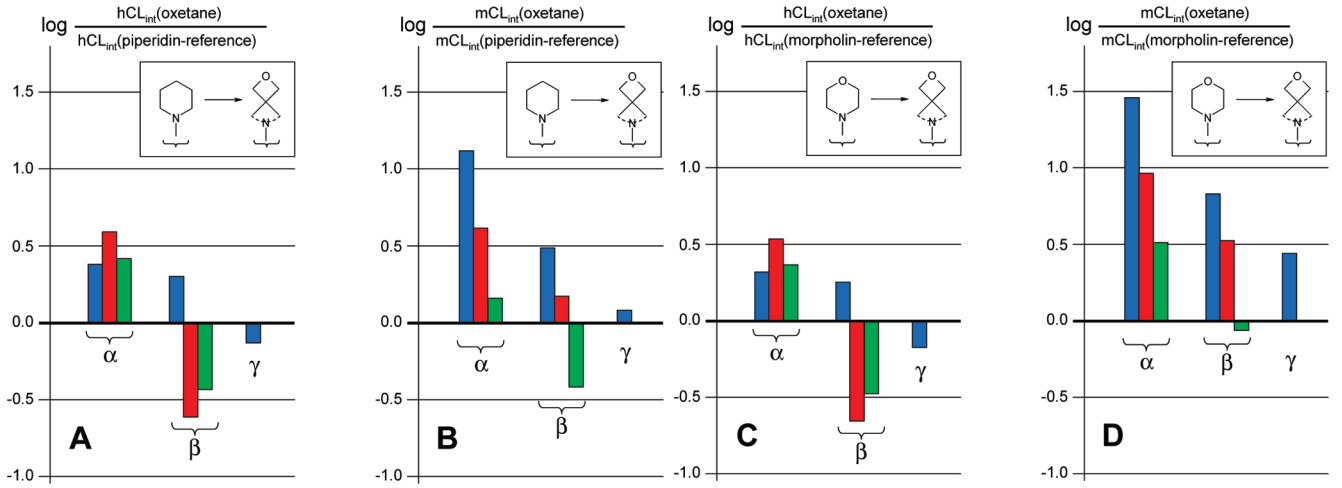

Figure 18. Logarithmic ratios of clearance rates (CL_{int}) for spirocyclic oxetane amines compared to piperidine derivative **34** in human (A) and mouse (B) liver microsomal assays, as obtained from corresponding value pairs in Table 1, and similar comparison for spirocyclic oxetane amines with morpholine derivative **33** in human (C) and mouse (D) liver microsomal assays. Bar color codes are blue, red, and green for piperidine, pyrrolidine, and azetidine derivatives, respectively.

enhanced by roughly 0.3 log units relative to those in Figure 18B because morpholine derivative **33** displays a lower clearance rate by a factor of 2 relative to its piperidine counterpart **34**. On the basis of the human microsomal assay data, all spirocyclic oxetaneamines could be of potential interest as building blocks for the replacement of a morpholine unit. Pyrrolidine **21** and, once again, the azetidine derivative **15** are particularly outstanding. Both feature the oxetane unit in β-position relative to the amine and are hardly metabolized.

An interesting electronic aspect emerges from the rigid superposition of **15** and **33**. Apart from the fact that the oxygen atom in **15** extends further out by ~1.3 Å, it is noted that the oxygen lone pair orbitals are in a plane orthogonal to the corresponding plane in the parent morpholine **33** (see Figure 17, right). This is in contrast with the superposition of **15** with the γ-piperidone derivative **31** (Figure 17, left) in which the oxygen lone pairs of the matched oxetane and carbonyl units are similarly disposed in space. These observations provide interesting opportunities in molecular design considering intermolecular interactions at a receptor site.

Preparation of Oxetanes. Ready synthetic access is critical for the practical applications of oxetanes. We felt that neither derivatization of commercially available oxetanes nor methods for their preparation had been sufficiently established to grant convenient access to the variety of 3-substituted oxetanes we envisioned for our studies.[47] Oxetan-3-one was investigated first for its use as a principal building block. Its rich chemistry yielded routes to a large number of compounds presented.[2] In the face of rising demand for oxetan-3-one and growing interest in oxetanes, we decided to reinvestigate[48] the oxidation of oxetan-3-ol, knowing that a high-yielding continuous process for its preparation had been in place.[49] Oxetan-3-ol can be oxidized under a number of conditions. However, purification and isolation of oxetan-3-one gave recurrent problems due to its volatility and hydrophilicity. After extensive experimentation and optimization[50] we found that treatment of oxetan-3-ol with phosphorus pentoxide, DMSO, and triethylamine[51] at −5 °C gives oxetan-3-one in 48% yield after distillation on a molar scale without requirement of aqueous workup (Scheme 2).

Scheme 2. Preparation of Acceptor Oxetanes from Oxetan-3-one (**43**)[a]

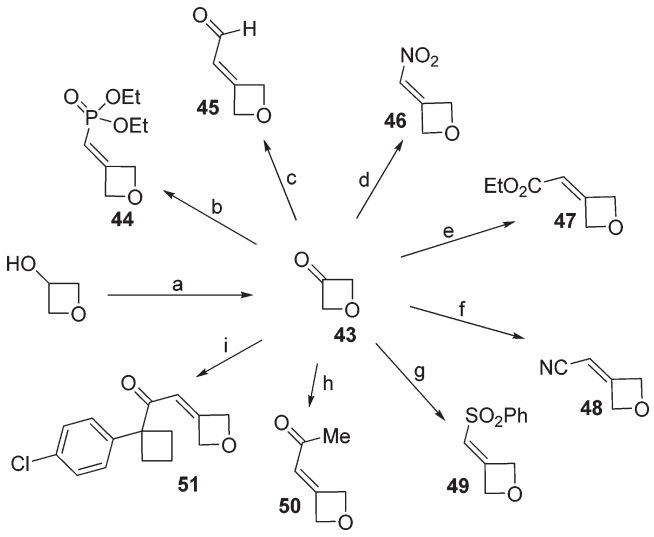

[a] (a) Me_2SO, P_4O_{10}, NEt_3, 48%; (b) Na·HC(P(O)(OEt)$_2$), 67%; (c) Ph_3P=CHCHO, 81%; (d) (1) $MeNO_2$, cat. NEt_3; (2) NEt_3, MsCl, 83%; (e) Ph_3P=$CHCO_2Et$, CH_2Cl_2, 95%; (f) Ph_3P=CHCN, 82%; (g) Li·HC(P(O)(OEt)$_2$)(SO_2Ph), 72%; (h) Ph_3P=CHC(O)Me, CH_2Cl_2, 95%; (i) Na·(4-chlorophenylcyclobutyl)-C(O)CHP(O)(OMe)$_2$, 90%.

Oxetan-3-one provides the starting point for almost all the chemistry we report. Most importantly, it serves as starting point for the preparation of a number of advanced oxetane building blocks with distinct Michael acceptor reactivity (Scheme 2). Reaction of oxetan-3-one with stable, commercially available ylides provides aldehyde **45**, α,β-unsaturated ester **47**, nitrile **48**,[52] and ketone **50** in good to excellent yields. Horner−Wadsworth−Emmons reactions furnish the corresponding phosphonate **44**, and sulfone **49** as well as the ketone **50**. Oxetan-3-one can also be condensed with nitromethane yielding nitroalkene **46**.

These compounds act as electrophiles in a number of conjugate addition reactions. They can be stored cold without noticeable decomposition over long periods of time. Their reactivity toward a large variety of nucleophiles provides ready access to a wide range of products.

Conjugate addition to acrylate **47** (Scheme 3) occurs smoothly with amines, cyanides, nitromethane, malonates, cuprates, and boronic acids, without concomitant formation of products resulting from 1,2-addition. This provides access to a variety of functional groups and structural motifs around the 3-substituted oxetane. Similar addition reactions of acrolein **45** (Scheme 4, left) with amines give unstable[53] β-aminoaldehydes that can be quenched in situ, for example, by reaction with phosphorus ylides. Addition of an arylboronic acid to **45** was successfully tested and shown to yield exclusively the 1,4-addition product **66**. Nitroolefin **46** reacts with a number of different carbon nucleophiles including acetaldehyde, aryllithium reagents, and aryl- and vinylboronic acids (Scheme 4, right). The yields of nucleophilic additions to **45** and **46** are lower than for the other conjugate acceptors because of side reactions in the case of aldehyde **45** or decomposition under basic reaction conditions. The functional groups present in the addition products of **45**−**47** are useful for further structural elaboration. However, the preparation of 3-methyloxetane derivatives is best effected through the use of a removable group. We could demonstrate that an addition product of aldehyde **45** can undergo decarbonylation with Wilkinson's catalyst.[54]

The use of vinylsulfone **49** permits a subsequent facile removal of the activation group, after nucleophilic addition, by treatment of the intermediate sulfone with Mg (Scheme 5). Initial results indicate that vinylsulfone **49** undergoes reaction with a variety of nucleophiles, including primary and secondary amines as well as arylboronic acids.

Scheme 3. Addition Reactions to Acrylate **47**[a]

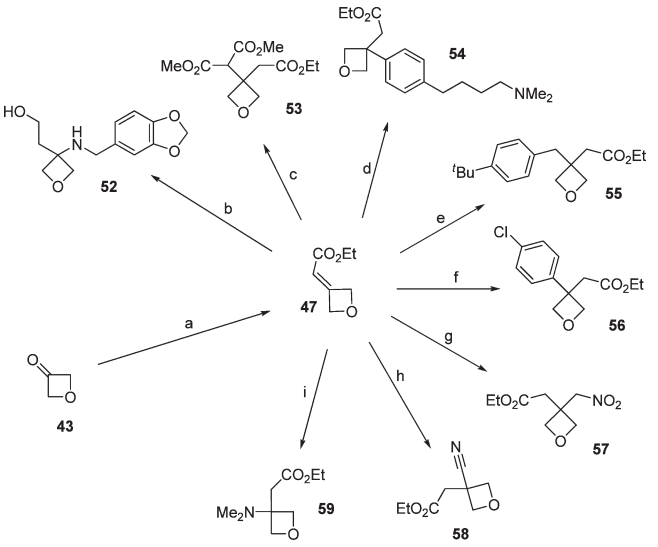

[a] (a) $Ph_3P{=}CHCO_2Et$, CH_2Cl_2, 95%; (b) piperonylamine, then $LiAlH_4$, Et_2O, 0 °C, 70%; (c) $H_2C(CO_2Me)$, NaH, THF, >82%; (d) (Me_2N)-$(CH_2)_4(C_6H_4)$-*p*-$B(OH)_2$, cat. $[Rh(cod)Cl]_2$, KOH, aq dioxane, room temp, 83%; (e) 4-^{t}BuBnMgBr, TMSCl, CuI, THF, −18 °C, 70%; (f) 4-Cl-PhB-$(OH)_2$, cat. $[Rh(cod)Cl]_2$, KOH, aq dioxane, room temp, 89%; (g) $MeNO_2$, cat. DBU, MeCN, 92%; (h) KCN, $(H_3C)_2C(OH)CN$, EtOH, 80%; (i) Me_2NH_2Cl, NEt_3, EtOH, quant.

Scheme 5. Addition Reactions to Vinylsulfone **49**[a]

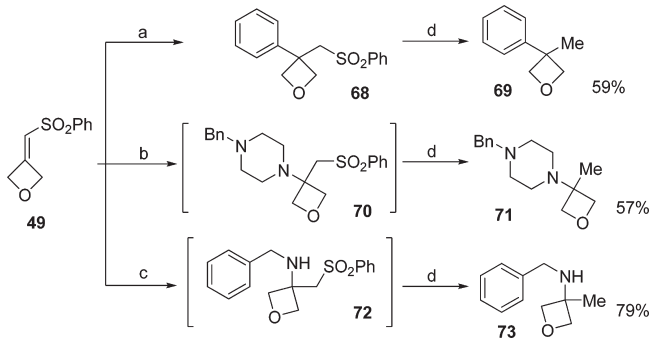

[a] (a) $PhB(OH)_2$, cat. $[Rh(cod)Cl]_2$, KOH, aq dioxane, room temp, 86%; (b) *N*-benzylpiperazine, MeOH; (c) benzylamine, MeOH; (d) Mg, MeOH, ultrasound, room temp.

Scheme 4. Addition Reactions to Acrolein **45** and Nitroolefin **46**[a]

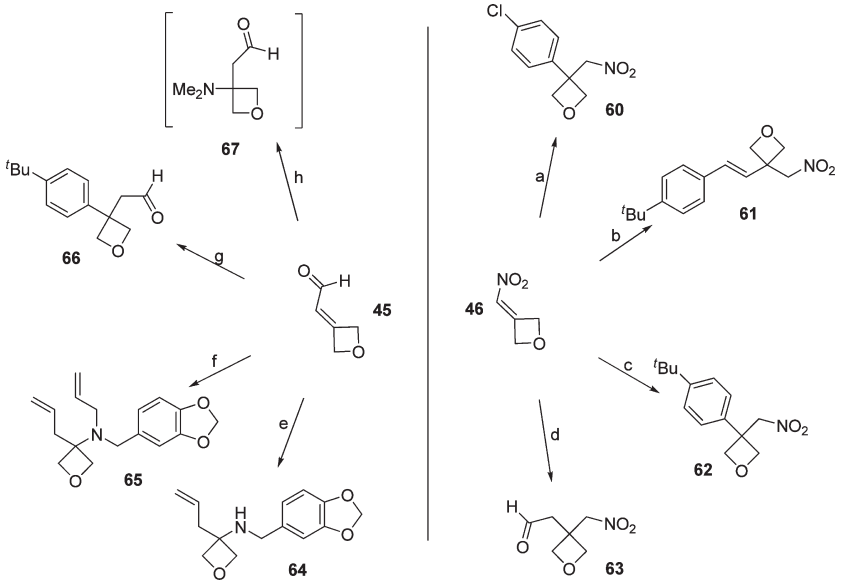

[a] (a) 4-Cl-PhLi, −78 °C, THF, 35%; (b) (*E*)-4-^{t}BuC_6H_4CHCHB$(OH)_2$, cat. $[Rh(cod)Cl]_2$, KOH, aq dioxane, room temp, 51%; (c) 4-^{t}BuPhB$(OH)_2$, KOH, cat. $[Rh(cod)Cl]_2$, aq dioxane, room temp, quant. (d) H_3CCHO, cat. pyrrolidine, 46%; (e) piperonylamine, cat. DBU, THF, −18 °C, then CH_2PPh_3; 29%; (f) piperonyl-N(H)allyl, cat. DBU, THF, −18 °C, then CH_2PPh_3, 53%; (g) 4-^{t}BuPhB$(OH)_2$, KOH, cat. $[Rh(cod)Cl]_2$, aq dioxane, room temp, 78%; (h) Me_2NH, cat. DBU, THF, −18 °C, used in situ without isolation.

The ability to utilize aryl- and vinylboronic acids as carbon nucleophiles in a simple procedure[55] allows us to tap into a vast reservoir of commercially available boronic acids and to access such oxetanes by parallel synthetic methods.

Conclusions

Grafting the small oxetane unit onto a molecular scaffold may have significant impacts on key physico- and biochemical properties. The possibility of introducing steric bulk without raising lipophilicity, while at the same time increasing aqueous solubility and keeping or even improving metabolic stability of the compound, renders oxetane incorporation an attractive concept in drug discovery. With ready synthetic access to oxetan-3-one and diverse electrophilic 3-methyleneoxetane intermediates established, the incorporation of oxetane into a large variety of structural contexts becomes straightforward.[56] Further research will focus on novel building blocks containing oxetane as well as other small heterocyclic units, their properties, and possible applications.

Experimental Section

General Information. Synthesis and characterization of compounds **1**, **2**, **4**, **6**, **8**, **10**, **37**−**40**, **45**−**47**, **54**, **55**, **61**, **66**, and **67** have been reported by us,[2a] as well as the synthesis and characterization of compounds **11**−**15**, **17**−**33**, **52**, **53**, **57**, **64**, and **65**.[2b] All nonaqueous reactions were carried out using oven-dried (90 °C) or flame-dried glassware under a positive pressure of dry nitrogen unless otherwise noted. Tetrahydrofuran, diethyl ether, toluene, and methylene chloride were purified by distillation and dried by passage over activated alumina under an argon atmosphere (H_2O content of <30 ppm, Karl−Fischer titration). Dioxane was distilled from calcium hydride under an inert atmosphere. Triethylamine was distilled from KOH under an atmosphere of dry nitrogen. All other commercially available reagents were used without further purification. Except if indicated otherwise, reactions were magnetically stirred and monitored by thin-layer chromatography using Merck silica gel 60 F_{254} or Merck aluminum oxide 60 F_{254} plates and visualized by fluorescence quenching under UV light. In addition, TLC plates were stained using ceric ammonium molybdate or potassium permanganate stain. Chromatographic purification of products (flash chromatography) was performed on E. Merck silica gel 60 (230−400 mesh) or Machery Nagel neutral aluminum oxide (Brockmann activity 1, deactivated with 6 wt % water) using a forced flow of eluant at 0.3−0.5 bar. Concentration under reduced pressure was performed by rotary evaporation at 40 °C at the appropriate pressure unless otherwise stated. Purified compounds were further dried for 12−72 h under high vacuum (0.01−0.05 Torr). Yields refer to chromatographically purified and spectroscopically pure compounds unless otherwise stated. Melting points were measured on a Büchi 510 apparatus. All melting points were measured in open capillaries and are uncorrected. NMR spectra were recorded on a Varian Mercury 300 spectrometer operating at 300 and 75 MHz for ^1H and ^{13}C acquisitions, respectively. Chemical shifts (δ) are reported in ppm with the solvent resonance as the internal standard relative to chloroform (δ 7.26) for 1H and chloroform (δ 77.0) for ^{13}C. All ^{13}C spectra were measured with complete proton decoupling. Data are reported as follows: s = singlet, d = doublet, t = triplet, q = quartet, m = multiplet; coupling constants are in Hz. IR spectra were recorded on a PerkinElmer Spectrum RXI FT-IR spectrophotometer. Absorptions are given in wavenumbers (cm^{-1}). Mass spectra were recorded by the MS Service at ETH Zürich: EI-MS (m/z), VG-TRIBRID spectrometer; MALDI-MS (m/z), IonSpec Ultima Fourier transform mass spectrometer. Elemental analyses (within 0.4% of calculated values, purity of $>99.6\%$) for the target compounds that form the basis of the study were performed at the Mikrolabor der ETH Zürich.

Determination of Solubility. For each compound, a sample of approximately 2 mg was added to ~150 μL of a 50 mM aqueous phosphate buffer and transferred to a standard 96-well plate at room temperature (22.5 ± 1 °C). The pH of each compound suspension was adjusted to pH 10 by using a concentrated NaOH solution, and the 96-well plate was placed on a plate shaker that agitated the suspensions overnight. On the next day the samples were filtered with a micronic filter plate (MSGVN2250) to separate the solid material from the solution. After confirmation of unchanged pH of the solutions by way of micro-pH-meter measurements, the solution concentrations were determined by calibrated HPLC. The calibrations were obtained by HPLC analysis of different concentrations of each compound in DMSO.

Determination of Lipophilicity ($\log D^{pH7.4}$). The high-throughput assay method is derived from the conventional "shake flask" method. The compound of interest is distributed between a 50 mM aqueous TAPSO buffer at pH 7.4 and 1-octanol. The distribution coefficient is then calculated from the difference in concentration in the aqueous phase before and after partitioning and the volume ratio of the two phases. To measure log D values within the range of −1 to 3.5, it is necessary to carry out the procedure at four different octanol/water ratios. The "one-phase-analysis" experiment starts with 2 or 9 μL of a pure DMSO solution of the compound, which is dispensed into, respectively, 38 or 171 μL of the aqueous buffer solution, bringing the compound concentration to approximately c = 0.5 mM. A small part of this solution is then analyzed by UV. The observed optical density corresponds to the concentration of the substance before partitioning. To a measured aliquot of the aqueous solution, a matching aliquot of 1-octanol is added, and the mixture is incubated by quiet shaking for 2 h at 23 ± 1 °C. The emulsion is allowed to stand overnight at the same temperature to ensure that the partition equilibrium is reached. Then, thorough centrifugation at 3000 rpm for 10 min is applied to separate the layers, and the concentration of the compound in the aqueous phase is determined again by measuring the UV absorption under the same conditions as the reference. For rather lipophilic compounds, this experimental procedure may be difficult to apply because of precipitation or limiting concentrations of the compounds. A new procedure has been successfully developed that relies on an immobilization of the octanol phase on a solid membrane support. By this measure the octanol volume can be reduced to 1 μL, which allows the measurement of highly lipophilic compounds with low water solubility.[57] The reported lipophilicity of **1** has been redetermined with this new method.

High-Throughput Measurement of Ionization Constants (pK_a). ProfilerSGA. Ionization constants are determined at 23 ± 1 °C by spectrophotometry using a ProfilerSGA SIRIUS instrument in buffered water solution at an ionic strength of 150 mM. To this end the UV spectrum of a compound is measured at different pH values. The solution of the sample is injected at constant flow rate into a flowing pH gradient. Changes in UV absorbance are monitored as a function of the pH gradient. The pK_a values are found and determined where the rate of change of absorbance is at a maximum. The pH gradient is established by proportionally mixing two flowing buffer solutions. The buffer solutions contain mixtures of weak acids and bases that are UV-spectroscopically transparent above 240 nm. It is necessary to calibrate the gradient in order to know exactly the pH at any given time. This is achieved by introducing standard compounds with known pK_a values. In cases where the pK_a could not be measured with the ProfilerSGA system because of an insufficient UV absorption of the compound, the pK_a values were measured by potentiometric titration (GLpKa). Internal validation studies (data not shown) proved that the difference between the pK_a values measured

with both instruments were within the experimental error of the individual experiments.

GLpKa. pK_a values with low UV absorption were determined by potentiometric titration (SIRIUS GLpKa analyzer) in aqueous solution containing 0.15 M KCl to adjust ionic strength. To measure pK_a of substances by the pH metric technique, a certain amount of sample was dissolved in the background electrolyte solution and acidified to pH 2 by addition of 0.5 M HCl. The solution was then titrated with standardized base (0.5 M KOH) to pH 12 at constant temperature (23 °C) under an atmosphere of argon to minimize absorption of atmospheric CO_2. The pK_a values were then calculated by shape analysis of the titration curve in comparison to the blank titration curve.

Determination of Metabolic Stability in Liver Microsomes. Microsomal incubations were carried out in 96-well plates in 200 μL of liver microsome incubation medium containing potassium phosphate buffer (50 mM, pH 7.4), $MgCl_2$ (10 mM), EDTA (1 mM), $NADP^+$ (2 mM), glucose 6-phosphate·$2H_2O$ (20 mM), glucose 6-phosphate dehydrogenase (4 units/mL) with 0.1 mg of liver microsomal protein per mL. Test compounds were incubated at 2 μM for up to 30 min at 37 °C under vortexing at 800 rpm. The reaction was stopped by transferring 30 μL incubation aliquots to 90 μL of ice-cold methanol. Levels of nonmetabolized drug were determined by high-performance liquid chromatography (HPLC) coupled with tandem mass spectrometry (LC/MS/MS). The system consisted of a Shimadzu binary gradient HPLC system, a Waters XTerra MS C18 column (1 mm × 50 mm), and a Sciex API 2000 mass spectrometer. A two-component mobile phase, pumped at 0.15 mL/min, contained the following solvents: solvent A (1% aqueous formic acid and MeOH 80:20) and solvent B (MeOH). An initial isocratic step of 0.5 min of solvent A was followed by a gradient of 0−80% solvent B within 1 min. Detection was performed in positive ion mode. The intrinsic pseudo-first-order clearance rate (CL_{int}) was determined from semilogarithmic plots of compound concentrations versus time.

Oxetan-3-one 43. Phosphorus pentoxide (184.5 g, 1.300 mols, 1.300 equiv) was suspended in 600 mL of CH_2Cl_2. Glassware need not be previously dried; the reaction is not air-sensitive. This suspension was cooled in an ice/salt bath to a temperature below 0 °C, before DMSO (106 mL, 1.50 mol, 1.50 equiv) was added followed by oxetan-3-ol (74.1 g, 1.00 mol, 1.00 equiv). The white dispersion was vigorously stirred, and once the temperature inside reached −5 °C, the addition of NEt_3 was started (307 mL, 2.20 mol, 2.20 equiv). The temperature should stay around 0 °C but not exceed 5 °C. Usually the addition takes 3−3.5 h. During the addition the mixture turned orange and became homogeneous. After the addition is finished the mixture is stirred for 5 min, before an amount of 600 mL of Et_2O is added. A phase separation occurred, the top phase containing the product. The two phases should be stirred for approximately 5 min. The top phase was then filtered using vacuum (~700 mbar) through a plug of silica gel (h = 7 cm, d = 13 cm) of which the top 2 cm were wetted with Et_2O (~150 mL). The bottom phase of the reaction mixture was thoroughly washed with five times 100 mL of diethyl ether, becoming very viscous. These were then also filtered through the plug, resulting in a total volume of filtrate of approximately 1.5 L. The filtrate was then transferred to a flask equipped with a stir bar and boiling chips, and the solvent was distilled off through a column filled with metal wire helices (joint 29, h 28 cm). The temperature of the oil bath should not exceed 60 °C. Once no more solvent was coming over, the column was replaced with a short path distillation apparatus and stirring at ambient pressure was continued until no more solvent came over. Then fractions were changed with the receiving flask being cooled with ice. The temperature of the oil bath was raised to 75 °C, and at the same time the pressure was slowly reduced to 100 mbar (~2 min from ambient pressure to 180 mbar, ~30 s from 180 to 100 mbar). Once this pressure was reached, fractions were changed and pure product came over with less than 2 wt % CH_2Cl_2. The pressure was further lowered slowly to 30 mbar and the distillation stopped when no more product came over. The intermediate fraction and the main fraction together contained 34.77 g of oxetan-3-one (48% yield). The spectroscopic data obtained are in accordance with the literature.[48] Oxetan-3-one should be stored in the freezer, where it solidifies.

Diethyl Oxetan-3-ylidenemethylphosphonate 44. To a suspension of sodium hydride (60% dispersion in mineral oil, 0.80 g, 20 mmol, 1.0 equiv) in 30 mL of dry THF was added a solution of tetraethyl methylenediphosphonate (5.0 mL, 20 mmol, 1.0 equiv) in 10 mL of dry THF dropwise at room temperature. After the mixture was stirred for 5 min, a solution of oxetan-3-one (1.4 g, 20 mmol, 1.0 equiv) in 5 mL of dry THF was added slowly. After the mixture was stirred for 2 h, the solvent was partially concentrated in vacuo, Et_2O (20 mL) and water (20 mL) were added, and the aqueous phase was extracted three times with Et_2O. The combined organic phases were dried over $MgSO_4$, filtered, and concentrated in vacuo and the residue was purified by flash chromatography (SiO_2, cyclohexane to remove mineral oil, then elute with EtOAc) to give 2.77 g of pure product (67% yield) as a colorless oil. R_f = 0.16 (SiO_2, 2/1 cyclohexane/EtOAc). ^{1}H NMR (300 MHz, $CDCl_3$): δ 5.49−5.35 (m, 3H), 5.29−5.21 (m, 2H), 4.14−3.97 (m, 4H), 1.37−1.26 (m, 6H). ^{13}C NMR (75 MHz, $CDCl_3$): δ 161.1, 106.9 (d, J = 189.3 Hz), 80.8 (d, J = 10.0 Hz), 79.5 (d, J = 27.6 Hz), 61.7 (d, J = 5.5 Hz), 16.3. ^{31}P NMR (121 MHz, $CDCl_3$): δ 15.8. HRMS (EI) calcd for $C_8H_{15}O_4P$ $[M-H]^{+\bullet}$ = 205.0625. Found: 205.0624.

(Oxetan-3-ylidene)acetonitrile 48. To a solution of oxetan-3-one (0.21 g, 3.0 mmol, 1.0 equiv) in 10 mL of dry CH_2Cl_2 was added cyanomethylenetriphenylphosphonium ylide (0.90 g, 3.0 mmol, 1.0 equiv) at room temperature. After the mixture was stirred for 6 h, the solvent was partially concentrated in vacuo and the mixture filtered through a plug of silica gel (2/1 to 1/1 pentane/Et_2O) to give 235 mg of pure product (82% yield) as slightly yellow crystals (mp = 56−58 °C). R_f = 0.30 (SiO_2, 2/1 cyclohexane/EtOAc). ^{1}H NMR (300 MHz, $CDCl_3$): δ 5.39 (m, 2H), 5.30 (m, 2H), 5.25 (td, 1H, J = 2.5 Hz, J = 5.0 Hz). ^{13}C NMR (75 MHz, $CDCl_3$): δ 163.3, 114.0, 90.8, 78.6, 78.4. HRMS (EI) calcd for C_5H_5NO $[M]^{+\bullet}$ 95.0371. Found: 95.0365.

3-(Benzenesulfonylmethylene)oxetane 49. To a solution methylphenylsulfone (5.0 g, 32 mmol, 1.0 equiv) in 150 mL of dry THF was added ^{n}BuLi (2.5 M in hexanes, 28 mL, 71 mmol, 2.2 equiv) at 0 °C over the course of 10 min. After the mixture was stirred for 30 min, chlorodiethylphosphonate (5.6 mL, 38 mmol, 1.2 equiv) was added dropwise and stirring was continued for 30 min before the mixture was cooled to −78 °C and oxetan-3-one (3.25 g, 45.1 mmol, 1.41 equiv) was added as a solution in 5 mL of dry Et_2O. After being stirred for 1.5 h, the mixture was filtered through a plug of silica gel to give 5.08 g of pure product (76% yield) as a colorless solid (mp = 51−53 °C). R_f = 0.25 (SiO_2, 2/1 cyclohexane/EtOAc). ^{1}H NMR (300 MHz, $CDCl_3$): δ 7.88 (d, 2H, J = 7.8 Hz), 7.66 (m, 1H), 7.57 (t, 2H, J = 7.3 Hz), 6.12 (m, 1H), 5.64 (m, 2H), 5.28 (m, 2H). ^{13}C NMR (75 MHz, $CDCl_3$): δ 156.2, 140.6, 133.7, 129.3, 127.2, 119.9, 79.6, 77.9. HRMS (EI) calcd for $C_{10}H_{10}O_3S$ $[M]^{+\bullet}$ 210.0351. Found: 210.0345.

1-(Oxetan-3-ylidene)propan-2-one 50. To a solution of oxetan-3-one (63 mg, 0.87 mmol, 1.0 equiv) in 8 mL of dry CH_2Cl_2 was added acetylmethylene triphenylphosphorane (0.33 g, 1.0 mmol, 1.3 equiv) at room temperature. The solution was stirred overnight and filtered through silica gel (4/1 to 2/1 pentane/Et_2O) to give 75 mg of pure product as a colorless oil in 77% yield. R_f = 0.16 (SiO_2, 2/1 cyclohexane/EtOAc). ^{1}H NMR (300 MHz, $CDCl_3$): δ 5.98 (m, 1H), 5.49 (m, 2H), 5.27 (m, 2H), 2.14 (s, 3H). ^{13}C NMR (75 MHz, $CDCl_3$): δ 196.4, 158.3, 118.0, 82.0, 78.9, 30.4. HRMS (EI) calcd for $C_6H_8O_2$ $[M]^{+\bullet}$ 112.0524. Found: 112.0519.

1-[1-(4-Chlorophenyl)cyclobutyl]-2-oxetan-3-ylidene]ethanone 51. To a solution of [2-[1-(4-chlorophenyl)cyclobutyl]-2-oxoethyl]phosphonic acid dimethyl ester (preparation described in Supporting Information, 0.95 g, 3.0 mmol, 1.0 equiv) in 10 mL

of dry THF was added sodium hydride (60% dispersion in mineral oil, 0.12 g, 3.0 mmol, 1.0 equiv) at 0 °C. After the mixture was stirred for 20 min, a solution of oxetan-3-one (0.22 g, 3.0 mmol, 1.0 equiv) in 1 mL of dry THF was added and the solution was stirred at 0 °C for 30 min. The solvent was concentrated in vacuo partially, toluene was added, and the mixture was put on a column (SiO_2, 20/1 to 4/1 cyclohexane/EtOAc) to give 750 mg of pure product (95% yield) as a colorless oil. The product is not stable at ambient temperature and rearranges to (5-(1-(4-chlorophenyl)cyclobutyl)furan-3-yl)methanol. R_f = 0.48 (SiO_2, 2/1 cyclohexane/EtOAc). ^{1}H NMR (300 MHz, $CDCl_3$): δ 7.32 (d, 2H, J = 8.6 Hz), 7.14 (d, 2H, J = 8.6 Hz), 5.88 (p, 1H, J = 2.3 Hz), 5.55 (m, 2H), 5.22 (m, 2H), 2.74 (m, 2H), 2.38 (m, 2H), 1.90 (m, 2H). ^{13}C NMR (75 MHz, $CDCl_3$): δ 197.7, 160.3, 141.0, 132.7, 128.8, 127.6, 113.5, 82.4, 79.0, 57.6, 30.3, 15.9. HRMS (EI) calcd for $C_{15}H_{15}ClO_2$ $[M]^{+\bullet}$ 262.0756. Found: 262.0752.

Ethyl 2-(3-(4-Chlorophenyl)oxetan-3-yl)acetate 56. To a solution of $[Rh(cod)Cl]_2$ (45 mg, 90 μmol, 0.04 equiv) in 7 mL of dioxane was added 1.5 M aqueous KOH (1.6 mL, 2.4 mmol, 1.0 equiv), and the yellow solution was stirred for 15 min. Then a mixture of 4-chlorobenzeneboronic acid (0.59 g, 3.7 mmol, 1.6 equiv) and acrylate **47** (0.33 g, 2.3 mmol, 1.0 equiv) in 7 mL of dioxane was slowly added, and the color of the solution turned to orange. After the mixture was stirred for 30 min at room temperature, additional 4-chlorobenzeneboronic acid (0.17 g, 1.1 mmol, 0.48 equiv) and 1.5 M aqueous KOH (0.50 mL, 0.75 mmol, 0.33 equiv) were added. The reaction was quenched after further 2 h by the addition of Et_2O (60 mL) and brine (40 mL). The aqueous phase was extracted two times with Et_2O (25 mL). The combined organic phases were dried over $MgSO_4$, filtered, and concentrated in vacuo. The residue was purified by flash chromatography (SiO_2, 8/1 to 2/1 cyclohexane/EtOAc) to give 0.33 g of pure product (56% yield) as slightly yellowish oil. R_f = 0.31 (SiO_2, 2/1 cyclohexane/EtOAc). ^{1}H NMR (300 MHz, $CDCl_3$): δ 7.31 (m, 2H), 7.12 (m, 2H), 4.96 (d, 2H, J = 6.2 Hz), 4.84 (d, 2H, J = 6.2 Hz), 4.01 (q, 2H, J = 7.1 Hz), 3.11 (s, 2H), 1.13 (t, 3H, J = 7.1 Hz). ^{13}C NMR (75 MHz, $CDCl_3$): δ 170.3 142.0 132.6, 128.6, 127.2, 81.7, 60.6, 45.1, 44.7, 14.2. HRMS (EI) calcd for $C_{13}H_{15}ClO_3$: $[M - CH_2O]^{+\bullet}$ 224.0595. Found: 224.0604.

(3-Cyanooxetan-3-yl)acetic Acid Ethyl Ester 58. To a solution of acrylate **47** (30 mg, 0.21 mmol, 1.0 equiv) in 2 mL of dry MeCN was added acetone cyanohydrin (16 μL, 0.42 mmol, 2.0 equiv), KCN (14 mg, 0.42 mmol, 2.0 equiv), and 18-crown-6 (0.11 g, 0.42 mmol, 2.0 equiv) at ambient temperature. After being stirred for 20 h, the mixture was concentrated in vacuo and the residue purified by flash chromatography (SiO_2, 4/1 cyclohexane/EtOAc) to give 29 mg pure product as a colorless oil. R_f = 0.10 (SiO_2, 2/1 cyclohexane/EtOAc). ^{1}H NMR (300 MHz, $CDCl_3$): δ 5.01 (d, 2H, J = 6.6 Hz), 4.55 (d, 2H, J = 6.6 Hz), 4.22 (q, 2H, J = 7.1 Hz), 3.08 (s, 2H), 1.29 (t, 3H, J = 7.2 Hz). ^{13}C NMR (75 MHz, $CDCl_3$): δ 168.6, 120.3, 78.1, 61.9, 40.2, 34.0, 14.3. HRMS (EI) calcd for $C_8H_{11}NO_3$ $[M]^{+\bullet}$ 169.0739. Found: 169.0739.

Ethyl 2-(3-(Dimethylamino)oxetan-3-yl)acetate 59. To a solution of acrylate **47** (1 M in Et_2O, 0.2 mL, 0.2 mmol, 1 equiv) in EtOH was added *N*,*N*-dimethylammmonium chloride (0.15 g, 1.9 mmol, 9.3 equiv), followed by NEt_3 (0.4 mL, 2.8 mmol, 14 equiv). After the mixture was stirred for 9 h at room temperature, the solvent was concentrated in vacuo and the residue partitioned between EtOAc and water. The aqueous phase was extracted three times with EtOAc, the combined organic phases were dried over $MgSO_4$, filtered, and concentrated in vacuo, and the residue was purified by flash chromatography (SiO_2, 7% MeOH in CH_2Cl_2, 0.1% NEt_3) to give 53 mg of pure product (135% yield) as a colorless oil. R_f = 0.66 (SiO_2, 10% MeOH in CH_2Cl_2, 0.1% NEt_3). ^{1}H NMR (300 MHz, $CDCl_3$): δ 4.57 (d, 2H, J = 6.2 Hz), 4.53 (d, 2H, J = 6.3 Hz), 4.13 (q, 2H, J = 7.1 Hz), 2.67 (s, 2H), 2.17 (s, 6H), 1.24 (t, 3H, J = 7.2 Hz). ^{13}C NMR (75 MHz, $CDCl_3$): δ 171.9, 78.9, 62.9, 60.9, 38.2, 34.4, 14.3. HRMS (EI) calcd for $C_9H_{17}NO_3$ $[M]^{+\bullet}$ 187.1208. Found: 187.1196. Calcd for $[M - CH_2O]^{+\bullet}$ 157.1098. Found: 157.1098. Anal. ($C_9H_{17}NO_3$) C, H, N.

3-(4-Chlorophenyl)-3-nitromethyloxetane 60. To 1-bromo-4-chlorobenzene (13.1 g, 68.3 mmol, 5.00 equiv) in 180 mL of dry THF was added ^{n}BuLi (2.5 M in hexanes, 24 mL, 60 mmol, 4.5 equiv) at −78 °C. The solution was stirred for 35 min before a solution of 3-nitromethyleneoxetane (**46**, 1.57 g, 13.7 mmol, 1.00 equiv) in 10 mL of dry THF was slowly added over 80 min. The mixture was then stirred for 40 min before it was poured on 150 mL of ice-cold 5% aqueous HCl. After the mixture was stirred for 15 min at 0 °C, the aqueous phase was extracted with CH_2Cl_2 three times (100 mL). The combined organic phases were dried over $MgSO_4$, filtered, and concentrated in vacuo. The residue was purified by flash chromatography (SiO_2, 8/1 to 2/1 cyclohexane/EtOAc), giving 1.20 g of >90% pure product (35% yield) as a colorless solid (mp = 115−117 °C). R_f = 0.39 (SiO_2, 2/1 cyclohexane/EtOAc). ^{1}H NMR (300 MHz, $CDCl_3$): δ 7.35 (d, 2H, J = 8.6 Hz), 7.03 (d, 2H, J = 8.6 Hz), 5.03 (d, 2H, J = 6.7 Hz), 5.00 (s, 2H), 4.90 (d, 2H, J = 6.8 Hz). ^{13}C NMR (75 MHz, $CDCl_3$): δ 138.0, 133.8, 129.1, 127.1, 82.0, 78.9, 46.8. HRMS (EI) calcd for $C_{10}H_{10}ClNO_3$ $[M]^{+\bullet}$ 227.0349. Found: 227.0343. Anal. ($C_{10}H_{10}ClNO_3$) C, H, N.

3-(4-*tert*-Butylphenyl)-3-(nitromethyl)oxetane 62. To a solution of $[Rh(cod)Cl]_2$ (5 mg, 9 μmol, 0.04 equiv) in 2 mL of dry dioxane was added 1.5 M aqueous KOH (0.17 mL, 0.25 mmol, 1.0 equiv), and the yellow solution was stirred for 3 min. Then 4-*tert*-butylbenzeneboronic acid (0.10 g, 0.50 mmol, 2.0 equiv) and nitroolefin **46** (29 mg, 0.25 mmol, 1.0 equiv) were consecutively added. After 2 h, the reaction mixture was partitioned between 120 mL of Et_2O and brine. The aqueous phase was extracted three times with Et_2O. The combined organic phases were dried over $MgSO_4$, filtered, and concentrated in vacuo. The residue was purified by flash chromatography (SiO_2, 8/1 cyclohexane/EtOAc) to give 65 mg (105% yield) of pure product as a colorless solid (mp = 86−87 °C). R_f = 0.39 (SiO_2, 2/1 cyclohexane/EtOAc). ^{1}H NMR (300 MHz, $CDCl_3$): δ 7.39 (d, J = 8.6 Hz, 2H), 7.04 (d, J = 8.6 Hz, 2H), 5.09 (d, J = 6.6 Hz, 2H), 5.01 (s, 2H), 4.92 (d, J = 6.7 Hz, 2H), 1.31 (s, 9H). ^{13}C NMR (75 MHz, $CDCl_3$): δ 151.0, 136.7, 126.1, 125.6, 82.4, 79.4, 47.0, 34.7, 31.4. HRMS (EI) calcd for $C_{14}H_{19}NO_3$ $[M]^{+\bullet}$ 249.1360. Found: 249.1360.

2-(3-(Nitromethyl)oxetan-3-yl)acetaldehyde 63. To a solution of nitroolefin **46** (0.45 g, 3.9 mmol, 1.0 equiv) and acetaldehyde (2.5 mL, 44 mmol, 11 equiv) in 15 mL of dry THF was added pyrrolidine (80 μL, 1.0 mmol, 0.26 equiv) slowly at room temperature. The mixture was stirred at room temperature overnight. CH_2Cl_2 (50 mL) was added, followed by 1 M aqueous HCl. The aqueous phase was extracted three times with CH_2Cl_2, the combined organic phases were dried over $MgSO_4$, filtered, concentrated in vacuo, and the residue was purified by flash chromatography (SiO_2, 2/1 to 1/1 cyclohexane/EtOAc) to give 0.29 g of pure product (46% yield) as a yellow oil that solidified in the freezer. R_f = 0.15 (SiO_2, 2/1 cyclohexane/EtOAc). ^{1}H NMR (300 MHz, $CDCl_3$): δ 9.74 (s, 1H), 4.92 (s, 2H), 4.63 (d, 2H, J = 7.1 Hz), 4.50 (d, 2H, J = 7.1 Hz), 3.18 (s, 2H). ^{13}C NMR (75 MHz, $CDCl_3$): δ 198.7, 78.8, 78.6, 47.3, 39.5. HRMS (EI) calcd for $C_6H_9NO_4$ $[M - CH_2NO_2]^{+\bullet}$ 99.0442; Found: 99.0446.

3-Phenyl-3-(phenylsulfonylmethyl)oxetane 68. To a solution of $[Rh(cod)Cl]_2$ (2 mg, 4 μmol, 0.05 equiv) in 1.6 mL of dry dioxane was added 1.5 M aqueous KOH (0.16 mL, 0.24 mmol, 1.0 equiv), and the yellow solution was stirred for 1 min. Then phenylboronic acid (58 mg, 0.48 mmol, 2.0 equiv) and phenylsulfone **49** (50 mg, 0.24 mmol, 1.0 equiv) were consecutively added. After 6 h, the sample showed 60% conversion, so more $[Rh(cod)Cl]_2$ (2 mg, 4 μmol, 0.05 equiv), KOH (0.16 mL, 0.24 mmol, 1.0 equiv), and phenylboronic acid (58 mg, 0.48 mmol, 2.0 equiv) were added to the mixture. After being stirred for 1 h, the reaction mixture was partitioned between Et_2O and brine.

The aqueous phase was extracted four times with Et_2O. The combined organic phases were dried over $MgSO_4$, filtered, and concentrated in vacuo. The residue was purified by flash chromatography (SiO_2, 20/1 to 2/1 cyclohexane/EtOAc) to give 60 mg of pure product (87% yield) as a colorless solid (mp = 162 °C). R_f = 0.21 (SiO_2, 2/1 cyclohexane/EtOAc). ^{1}H NMR (300 MHz, $CDCl_3$): δ 7.57−7.41 (m, 3H), 7.38−7.28 (m, 2H), 7.25−7.14 (m, 3H), 7.06 (m, 2H), 5.07 (d, J = 6.5 Hz, 2H), 4.95 (d, J = 6.6 Hz, 2H), 4.04 (s, 2H). ^{13}C NMR (75 MHz, $CDCl_3$): δ 140.4, 140.3, 133.1, 128.8, 128.5, 127.3, 127.2, 126.3, 80.9, 65.1, 45.8. HRMS (EI) calcd for $C_{16}H_{16}O_3S$ $[M - CH_2O]^{+\bullet}$ 258.0709. Found: 258.0710.

3-Methyl-3-phenyloxetane 69. To a solution of sulfone **68** (0.25 g, 0.86 mmol, 1.0 equiv) in 20 mL of MeOH was added Mg granulate (1.0 g, 42 mmol, 48 equiv), and the mixture was stirred for 2 min in an ultrasound bath. Stirring was continued for 12 h, when a sample in the NMR showed full conversion to product. Et_2O (40 mL) was added followed by $Na_2SO_4 \cdot 10H_2O$. After being stirred for 15 min, the mixture was filtered, the filtrate dried over $MgSO_4$, filtered, evaporated, and the residue filtered through a plug of silica gel. The combined filtrate was evaporated and the residue distilled bulb-to-bulb at 200 mbar to give 76 mg of pure product (59% yield) as a colorless oil. R_f = 0.21 (SiO_2, 2/1 cyclohexane/EtOAc). ^{1}H NMR (300 MHz, $CDCl_3$): δ 7.39−7.29 (m, 3H), 7.23−7.12 (m, 2H), 4.96 (d, J = 5.7 Hz, 2H), 4.61 (d, J = 5.2 Hz, 2H), 1.71 (s, 3H). ^{13}C NMR (75 MHz, $CDCl_3$): δ 146.2, 128.4, 126.1, 124.9, 83.7, 43.5, 28.1. HRMS (EI) calcd for $C_{10}H_{12}O$ $[M - C_6H_5]^{+\bullet}$ 71.0497. Found: 71.0854.

1-Benzyl-4-(3-methyloxetan-3-yl)piperazine 71. A solution of *N*-benzypiperazine (0.19 mL, 1.1 mmol, 1.1 equiv) and sulfone **49** (0.21 g, 1.0 mmol, 1.0 equiv) in 5 mL of MeOH was stirred for 20 h at 50 °C. Then magnesium turnings (0.13 g, 5.0 mmol, 5.0 equiv) were added to the solution and the mixture was stirred for 30 s in an ultrasound bath to start the reaction (slight bubbling). After the mixture was stirred overnight, more magnesium (0.13 g, 5.0 mmol, 5.0 equiv) was added and stirring was continued for 16 h. Et_2O was added, followed by $Na_2SO_4 \cdot 10H_2O$, and the mixture was stirred for 20 min, filtered, dried over Na_2SO_4, filtered, concentrated in vacuo and the residue purified by flash chromatography (nAl_2O_3, 20/1 to 4/1 cyclohexane/EtOAc) to give 141 mg of pure product (57% yield) as a yellowish oil. R_f = 0.39 (Al_2O_3, 2/1 cyclohexane/EtOAc). ^{1}H NMR (300 MHz, $CDCl_3$): δ 7.35−7.23 (m, 5H), 4.57 (d, J = 5.3 Hz, 2H), 4.20 (d J = 5.3 Hz, 2H), 3.51 (s, 2H), 2.51 (s, 4H), 2.45−2.33 (m, 4H), 1.37 (s, 3H). ^{13}C NMR (75 MHz, $CDCl_3$): δ 137.8, 129.0, 128.0, 126.9, 81.4, 63.0, 60.0, 53.1, 45.1, 15.3. HRMS (EI) calcd for $C_{15}H_{22}N_2O$ $[M - CH_2O]^{+\bullet}$ 216.1621. Found: 216.1621.

***N*-Benzyl-3-methyloxetan-3-amine 73.** A solution of benzylamine (0.12 mL, 1.1 mmol, 1.1 equiv) and sulfone **49** (0.21 g, 1.0 mmol, 1.0 equiv) in 5 mL of MeOH was stirred for 3 h at 50 °C. Then magnesium turnings (0.13 g, 5.0 mmol, 5.0 equiv) were added to the solution, and the mixture was stirred for 30 s in an ultrasound bath to start the reaction (slight bubbling). After the mixture was stirred overnight, more magnesium (0.13 g, 5.0 mmol, 5.0 equiv) was added and stirring was continued for 16 h. Et_2O was added, followed by $Na_2SO_4 \cdot 10H_2O$, and the mixture was stirred for 20 min, filtered, dried over Na_2SO_4, filtered, concentrated in vacuo and the residue purified by flash chromatography (nAl_2O_3, 20/1 to 4/1 cyclohexane/EtOAc) to give 140 mg of pure product (79% yield) as a yellowish oil. R_f = 0.50 (Al_2O_3, 2/1 cyclohexane/EtOAc). ^{1}H NMR (300 MHz, $CDCl_3$): δ 7.39−7.22 (m, 5H), 4.57 (d, J = 6.6, 2H), 4.41 (d, J = 6.6, 2H), 3.79 (s, 2H), 1.65 (s, 1H), 1.55 (s, 3H). ^{13}C NMR (75 MHz, $CDCl_3$): δ 140.0, 128.4, 127.9, 127.0, 83.1, 57.5, 47.9, 23.6. HRMS (EI) calcd for $C_{11}H_{15}NO$ $[M - CH_3O]^{+\bullet}$ 146.0965. Found: 146.0966.

Acknowledgment. We thank F. Hoffmann-La Roche AG for support of this research and Syngenta for the donation of oxetan-3-ol. We are very indebted to Dr. Manfred Kansy and Dr. Stefanie Bendels for valuable discussions of physicochemical data. We also thank Dr. Bernd W. Schweizer and André Alker for the performance of X-ray structure analyses.

Supporting Information Available: Experimental procedures for nonoxetane containing intermediates and reference compounds **3**, **5**, **7**, **9**. This material is available free of charge via the Internet at http://pubs.acs.org.

References

(1) Leeson, P. D.; Springthorpe, B. The influence of drug-like concepts on decision-making in medicinal chemistry. *Nat. Rev. Drug Discovery* **2007**, *6* (11), 881–890.

(2) (a) Wuitschik, G.; Rogers-Evans, M.; Müller, K.; Fischer, H.; Wagner, B.; Schuler, F.; Polonchuk, L.; Carreira, E. M. Oxetanes as promising modules in drug discovery. *Angew. Chem., Int. Ed.* **2006**, *45* (46), 7736. (b) Wuitschik, G.; Rogers-Evans, M.; Buckl, A.; Bernasconi, M.; Märki, M.; Godel, T.; Fischer, H.; Wagner, B.; Parrilla, I.; Schuler, F.; Schneider, J.; Alker, A.; Schweizer, W. B.; Müller, K.; Carreira, E. M. Spirocyclic oxetanes: synthesis and properties. *Angew. Chem., Int. Ed.* **2008**, *47* (24), 4512–4515.

(3) Within this framework, oxetanes offer an entry into significant target property modifications as well as securing an immediate ip advantage as observed with ~150 pharma patents in 2009 claiming 3-substituted oxetanes. Recent examples include the following: (a) Preparation of Heteroarylphenylamine Derivatives for Use as Amyloid Beta Modulators. WO 2009103652, 2009; F. Hoffmann-La Roche AG, Switzerland. (b) Biphenyls and Biheteroaryls End-Capped with Peptide Derivatives as Hepatitis C Virus Inhibitors. WO 2009102318, 2009; Bristol-Myers Squibb Co. (c) Triazolium Salts as PAR1 Inhibitors, Production Thereof, and Use as Medicaments. WO 2009097971, 2009; Sanofi-Aventis, France. (d) Preparation of 1,2-Disubstituted-4-benzylamino-pyrrolidine Derivatives as CETP Inhibitors. WO 2009071509, **2009**; Novartis A.-G., Switzerland. (e) Preparation of [1H-Pyrazolo[3,4-b]pyridin-4-yl]phenyl as Protein Kinase C-Theta Inhibitors. WO 2009073300, **2009**; Vertex Pharmaceuticals Incorporated. (f) Preparation of Phenyloxetane Derivatives for Treatment of Autoimmune System Diseases. WO 2009068682, **2009**; Novartis AG, Switzerland.

(4) Recently, independent from us, studies have emerged further exploring the synthetic accessibility of 3-substituted oxetanes: (a) Duncton, M. A. J.; Estiarte, M. A.; Tan, D.; Kaub, C.; O'Mahony, D. J. R.; Johnson, R. J.; Cox, M.; Edwards, W. T.; Wan, M.; Kincaid, J.; Kelly, M. G. Preparation of aryloxetanes and arylazetidines by use of an alkyl−aryl Suzuki coupling. *Org. Lett.* **2008**, *10* (15), 3259–3262. (b) Duncton, M. A. J.; Estiarte, M. A.; Johnson, R. J.; Cox, M.; O'Mahony, D. J. R.; Edwards, W. T.; Kelly, M. G. Preparation of heteroaryloxetanes and heteroarylazetidines by use of a Minisci reaction. *J. Org. Chem.* **2009**, *74* (16), 6354–6357.

(5) More than 10% of all launched drugs contain at least one *gem*-dimethyl group, highlighting its relevance for drug discovery (Prous Science Integrity, May 2008).

(6) (a) Magnin et al. reported the protection of an α-(acylamino)nitrile from hydrolysis by introduction of steric bulk in the aminonitrile part. Magnin, D. R.; Robl, J. A.; Sulsky, R. B.; Augeri, D. J.; Huang, Y. T.; Simpkins, L. M.; Taunk, P. C.; Betebenner, D. A.; Robertson, J. G.; Abboa-Offei, B. E.; Wang, A. Y.; Cap, M.; Xin, L.; Tao, L.; Sitkoff, D. F.; Malley, M. F.; Gougoutas, J. Z.; Khanna, A.; Huang, Q.; Han, S. P.; Parker, R. A.; Hamann, L. G. Synthesis of novel potent dipeptidyl peptidase IV inhibitors with enhanced chemical stability: interplay between the N-terminal amino acid alkyl side chain and the cyclopropyl group of alpha-aminoacyl-L-*cis*-4,5-methanoprolinenitrile-based inhibitors. *J. Med. Chem.* **2004**, *47* (10), 2587–2598. (b) For an example where an imidazoline is protected from hydrolyis by bulky substituents, seethe following: von Rauch, M.; Schlenk, M.; Gust, R. Effects of C2-alkylation, N-alkylation, and N,N′-dialkylation on the stability and estrogen receptor interaction of (4R,5S)/(4S,5R)-4,5-bis(4-hydroxyphenyl)-2-imidazolines. *J. Med. Chem.* **2004**, *47* (4), 915–927.

(7) (a) Manoury, P. M.; Binet, J. L.; Rousseau, J.; Lefevreborg, F. M.; Cavero, I. G. Synthesis of a series of compounds related to betaxolol, a new beta-1-adrenoceptor antagonist with a pharmacological and pharmacokinetic profile optimized for the treatment of chronic cardiovascular-diseases. *J. Med. Chem.* **1987**, *30* (6), 1003–1011. (b) For an example where steric bulk reduced susceptibility toward imide cleavage, see the following: Borthwick, A. D.; Davies, D. E.; Ertl, P. F.; Exall, A. M.; Haley, T. M.; Hart, G. J.; Jackson, D. L.; Parry, N. R.; Patikis, A.; Trivedi, N.; Weingarten, G. G.; Woolven, J. M.

Design and synthesis of pyrrolidine-5,5′-trans-lactams (5-oxo-hexahydropyrrolo[3,2-b]pyrroles) as novel mechanism-based inhibitors of human cytomegalovirus protease. 4. Antiviral activity and plasma stability. *J. Med. Chem.* **2003**, *46* (21), 4428–4449. (c) Addition of steric bulk can help to reduce glucuronidation (phase II metabolism): Madsen, P.; Ling, A.; Plewe, M.; Sams, C. K.; Knudsen, L. B.; Sidelmann, U. G.; Ynddal, L.; Brand, C. L.; Andersen, B.; Murphy, D.; Teng, M.; Truesdale, L.; Kiel, D.; May, J.; Kuki, A.; Shi, S. H.; Johnson, M. D.; Teston, K. A.; Feng, J.; Lakis, J.; Anderes, K.; Gregor, V.; Lau, J. Optimization of alkylidene hydrazide based human glucagon receptor antagonists. Discovery of the highly potent and orally available 3-cyano-4-hydroxybenzoic acid [1-(2,3,5,6-tetramethylbenzyl)-1H-indol-4-ylmethylene]hydrazide. *J. Med. Chem.* **2002**, *45* (26), 5755–5775.

(8) For examples, see the following: (a) Duffy, J. L.; Rano, T. A.; Kevin, N. J.; Chapman, K. T.; Schleif, W. A.; Olsen, D. B.; Stahlhut, M.; Rutkowski, C. A.; Kuo, L. C.; Jin, L. X.; Lin, J. H.; Emini, E. A.; Tata, J. R. HIV protease inhibitors with picomolar potency against PI-resistant HIV-1 by extension of the P-3 substituent. *Bioorg. Med. Chem. Lett.* **2003**, *13* (15), 2569–2572. (b) Ahmad, S.; Doweyko, L. M.; Dugar, S.; Grazier, N.; Ngu, K.; Wu, S. C.; Yost, K. J.; Chen, B. C.; Gougoutas, J. Z.; DiMarco, J. D.; Lan, S. J.; Gavin, B. J.; Chen, A. Y.; Dorso, C. R.; Serafino, R.; Kirby, M.; Atwal, K. S. Arylcyclopropanecarboxyl guanidines as novel, potent, and selective inhibitors of the sodium hydrogen exchanger isoform-1. *J. Med. Chem.* **2001**, *44* (20), 3302–3310.

(9) Vinyl-substituted carbonyl compounds are not present in marketed drugs (Prous Science Integrity, May 2008).

(10) Search on MDL Metabolite Database and Prous Science Integrity (May 2008) for metabolic reactions yielded no hits.

(11) Prous Science Integrity, May 2008: Substructure search for launched compounds containing a morpholine unit: (a) McKillop, D.; McCormick, A. D.; Miles, G. S.; Phillips, P. J.; Pickup, K. J.; Bushby, N.; Hutchison, M. In vitro metabolism of gefitinib in human liver microsomes. *Xenobiotica* **2004**, *34* (11), 983–1000. (b) Balani, S. K.; Pitzenberger, S. M.; Schwartz, M. S.; Ramjit, H. G.; Thompson, W. J. Metabolism of L-689,502 by rat-liver slices to potent HIV-1 protease inhibitors. *Drug Metab. Dispos.* **1995**, *23* (2), 185–189. (c) Hayashi, T.; Aoyama, M.; Fukuda, M.; Ohki, M.; Kishikawa, T. Metabolism of 4-ethoxy-2-methyl-5-morpholino-3(2H)-pyridazinone (M73101), a new anti-inflammatory agent. 2. Species-differences of metabolism and excretion. *Chem. Pharm. Bull.* **1979**, *27* (2), 317–325. (d) Giraldi, P. N.; Tosolini, G. P.; Dradi, E.; Nannini, G.; Longo, R.; Meinardi, G.; Monti, G.; Carneri, I. D. Studies on antiprotozoans. 3. Isolation, identification and quantitative determination in humans of metabolites of a new trichomonacidal agent. *Biochem. Pharmacol.* **1971**, *20* (2), 339. (e) Betts, A.; Atkinson, F.; Gardner, I.; Fox, D.; Webster, R.; Beaumont, K.; Morgan, P. Impact of physicochemical and structural properties on the pharmacokinetics of a series of alpha 1(L)-adrenoceptor antagonists. *Drug Metab. Dispos.* **2007**, *35* (8), 1435–1445. (f) Jauch, R.; Griesser, E.; Oesterhelt, G.; Arnold, W.; Meister, W.; Ziegler, W. H.; Guentert, T. W. Biotransformation of moclobemide in humans. *Acta Psychiatr. Scand., Suppl.* **1990**, *360*, 87. (g) Coutts, R. T.; Jamali, F.; Malek, F.; Peliowski, A.; Finer, N. N. Urinary metabolites of doxapram in premature neonates. *Xenobiotica* **1991**, *21* (10), 1407–1418.

(12) A search in the Cambridge Structural Database (CSD), version 5.30 (November 2008), for oxetanes, unsubstituted in 2- and 4-positions and carrying only one or two hydrogen atoms or CH_2X groups in the 3-position (X = H, C, N, O, F, Si, P, S, Cl, Br, I) yielded nine entries for 3,3-disubstituted and two entries for unsubstituted oxetane.

(13) All references to the CSD in this paper refer to the Cambridge Structural Database, version 5.30 (November 2008).

(14) Chan, S. I.; Zinn, J.; Fernandez, J.; Gwinn, W. D.; Trimethylene Oxide, I. Microwave spectrum, dipole moment, and double minimum vibration. *J. Chem. Phys.* **1960**, *33* (6), 1643–1655.

(15) On the basis of these results, one would predict that ring closures leading to spirocyclic oxetanes are faster than for their *gem*-dimethyl analogues.

(16) For ketones and *gem*-dimethyl derivatives, R was defined as tetrahedral carbon. For oxetane derivatives, R was relaxed to allow for elements C, N, O, Si, P, S, F, Cl, Br, I.

(17) Edward, J. T.; Farrell, P. G.; Shahidi, F. Partial molar volumes of organic compounds in water. Part 1. Ethers, ketones, esters, and alcohols. *J. Chem. Soc., Faraday Trans. 1* **1977**, *73* (5), 705–714.

(18) Zhou, T. L.; Battino, R. Partial molar volumes of 13 gases in water at 298.15 and 303.15 K. *J. Chem. Eng. Data* **2001**, *46* (2), 331–332.

(19) While the partial molar volume of formaldehyde in water is not available, an upper limit can be estimated from the partial molar volume of ethylene in water, 45.4 cm^3/mol at 25 °C (ref 16).

(20) Metabolite determination for compound **6** showed that its main metabolites are the corresponding *N*-oxide, a benzylic alcohol, and the primary alcohol resulting from attack on the *tert*-butyl group.

(21) Fischer, H.; Kansy, M.; Bur, D. CAFCA: a novel tool for the calculation of amphiphilic properties of charged drug molecules. *Chimia* **2000**, *54* (11), 640–645.

(22) Cavalli, A.; Poluzzi, E.; De Ponti, F.; Recanatini, M. Toward a pharmacophore for drugs inducing the long QT syndrome: Insights from a CoMFA study of HERG K+ channel blockers. *J. Med. Chem.* **2002**, *45* (18), 3844–3853.

(23) Compared to what was to be expected based on the pK_a shifts in the open chain, the extent to which this calculated decrease is realized in various heterocycles is as follows: piperidine **27**, 77%; pyrrolidine **21**, 62%; azetidine **15**, 39% of the theoretical value. Theoretical values were calculated by adding the appropriate pK_a shifts of the open chain, e.g., for piperidine **24**, $\Delta pK_a(\beta) + \Delta pK_a(\delta)$.

(24) Morgenthaler, M.; Schweizer, E.; Hoffmann-Roder, A.; Benini, F.; Martin, R. E.; Jaeschke, G.; Wagner, B.; Fischer, H.; Bendels, S.; Zimmerli, D.; Schneider, J.; Diederich, F.; Kansy, M.; Müller, K. Predicting properties and tuning physicochemical in lead optimization: amine basicities. *ChemMedChem* **2007**, *2* (8), 1100–1115.

(25) NMR analysis of the protonated pyrrolidine **18** did not give a clear picture of the preferred conformation. This is probably due to the high conformational flexibility of five-membered rings.

(26) Greig, I. R.; Tozer, M. J.; Wright, P. T. Synthesis of cyclic sulfonamides through intramolecular Diels−Alder reactions. *Org. Lett.* **2001**, *3* (3), 369–371.

(27) Venkatachalam, T. K.; Sudbeck, E.; Uckun, F. M. Structural influence on the anisotropic intermolecular hydrogen bonding in solid state of substituted thioureas: evidence by X-ray crystal structure. *J. Mol. Struct.* **2004**, *687* (1−3), 45–56.

(28) Müller, K.; Faeh, C.; Diederich, F. Fluorine in pharmaceuticals: looking beyond intuition. *Science* **2007**, *317* (5846), 1881–1886.

(29) Böhm, H. J.; Banner, D.; Bendels, S.; Kansy, M.; Kuhn, B.; Müller, K.; Obst-Sander, U.; Stahl, M. Fluorine in medicinal chemistry. *ChemBioChem* **2004**, *5* (5), 637–643.

(30) Berthelot, M.; Besseau, F.; Laurence, C. The hydrogen-bond basicity pKHB scale of peroxides and ethers. *Eur. J. Org. Chem.* **1998**, No. 5, 925–931. The equilibrium concentrations were determined by measuring the absorbances of the O−H stretching of 4-fluorophenol for different initial base concentrations.

(31) Brandon, M.; Tamres, M.; Searles, S. The iodine complexes of some saturated cyclic ethers. 1. The visible region. *J. Am. Chem. Soc.* **1960**, *82* (9), 2129–2134.

(32) Sisler, H. H.; Perkins, P. E. Molecular addition compounds of dinitrogen tetroxide. 6. Binary systems with trimethylene oxide, 2,5-dimethyl tetrahydrofuran and 1,3-dioxolane. *J. Am. Chem. Soc.* **1956**, *78* (6), 1135–1136.

(33) Bennett, G. M.; Philip, W. G. The influence of structure on the solubilities of ethers. Part II. Some cyclic ethers. *J. Chem. Soc.* **1928**, 1937–1942.

(34) Korolev, A. M.; Eremenko, L. T.; Meshikhina, L. V.; Eremenko, I. L.; Aleksandrov, G. G.; Konovalova, N. P.; Lodygina, V. P. *Izv. Akad. Nauk SSSR, Ser. Khim.* **2003**, 1763.

(35) IVAGUH: Korolev, A. M.; Eremenko, L. T.; Meshikhina, L. V.; Eremenko, I. L.; Aleksandrov, G. G.; Konovalova, N. P.; Lodygina, V. P.Synthesis and study of organic nitrates of heterofunctional series 5. Synthesis of 3,3-bis(hydroxymethyl)oxetane mono- and dinitrates and 2,2-bis(hydroxymethyl)propane-1,3-diol (pentaerythritol) mono- and dinitrates. *Russ. Chem. Bull.* **2003**, *52* (8), 1859–1863.

(36) CCDC 721350 (**41**) and CCDC 721113 (**42**) contain the supplementary crystallographic data for this paper. These data can be obtained free of charge from the Cambridge Crystallographic Data Centre via www.ccdc.cam.ac.uk/data_request/cif.

(37) Data taken from ref 36. For a definition of $\log K_{HB}$ and the method used to determine it, see the following: Berthelot, M.; Besseau, F.; Laurence, C. The hydrogen-bond basicity pKHB scale of peroxides and ethers. *Eur. J. Org. Chem.* **1998**, No. 5, 925–931.

(38) For the H-bonding affinity of oxetanes, see ref 37. For related studies with a variety of carbonyl compounds, see the following: (a) Besseau, F.; Lucon, M.; Laurence, C.; Berthelot, M. Hydrogen-bond basicity pK(HB) scale of aldehydes and ketones. *J. Chem. Soc., Perkin Trans. 2* **1998**, No. 1, 101–107. (b) Besseau, F.; Laurence, C.; Berthelot, M. Hydrogen-bond basicity of esters, lactones and carbonates. *J. Chem. Soc., Perkin Trans. 2* **1994**, No. 3, 485–489. (c) Lequestel, J. Y.; Laurence, C.; Lachkar, A.; Helbert, M.; Berthelot, M. Hydrogen-bond basicity of secondary and tertiary amides, carbamates, ureas and lactams. *J. Chem. Soc., Perkin Trans. 2* **1992**, No. 12, 2091–2094.

(39) Searles, S. The reaction of trimethylene oxide with Grignard reagents and organolithium compounds. *J. Am. Chem. Soc.* **1951**, *73* (1), 124–125.

(40) Pritchard, J. G.; Long, F. A. The kinetics of the hydrolysis of trimethylene oxide in water, deuterium oxide and 40-percent aqueous dioxane. *J. Am. Chem. Soc.* **1958**, *80* (16), 4162–4165.
(41) Wuitschik, G. Oxetanes in Drug Discovery. Ph.D. Dissertation, ETH Zurich, Zurich, Switzerland, **2008**; DOI: 10.3929/ethz-a-005697432 (http://e-collection.ethbib.ethz.ch/view/eth:30903).
(42) Ringner, B.; Sunner, S.; Watanabe, H. Enthalpies of combustion and formation of some 3,3-disubstituted oxetanes. *Acta Chem. Scand.* **1971**, *25* (1), 141.
(43) DEREK for Windows toxicity prediction (LHASA Ltd., www.lhasalimited.org) will not pick up 3-substituted oxetanes because there is not enough data available to generate a reliable rule. However, studies about the formation of glutathione conjugates by Duncton et al. (ref 4a) provide additional evidence that the oxetan-3-yl chemotype is attractive for medicinal chemistry. Also, the fluoro-oxetane below (H3 antagonist program) was determined as Ames and MNT negative (private communication of one of the authors (M.R.-E.) with Dr. J. M. Plancher (Roche)):

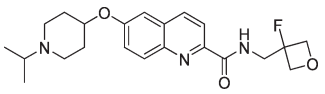

(44) None of these carbonyl compounds show significant decomposition during exposure to buffers of different pH at 37 °C for 2 h; however, both β-amino ketones tend to turn into insoluble products upon storage in the refrigerator. At ambient temperature, decomposition occurs in less than 1 day.
(45) The model was obtained from the X-ray structure, as retrieved from CSD, reference code CERBEH: Sax, M.; Ebert, K.; Schepmann, D.; Wibbeling, B.; Wunsch, B. Synthesis and NMDA-receptor affinity of 4-oxo-dexoxadrol derivatives. *Bioorg. Med. Chem.* **2006**, *14* (17), 5955–5962.
(46) The model obtained from the X-ray structure, as retrieved from CSD, reference code HOTSEO: Crisp, G. T.; Jensen, W. P.; Tiekink, E. R. T.; Turner, P. D. Crystal structure of 2,6-di-(morpholinomethyl)phenol, $C_{16}H_{24}N_2O_3$. *Z. Kristallogr.—New Cryst. Struct.* **1999**, *214* (4), 521–522.
(47) Wuitschik, G.; Carreira, E. M.; Rogers-Evans, M.; Müller, K. Oxetan-3-one: Chemistry and Synthesis. In *Process Chemistry in the Pharmaceutical Industry*; Gadamasetti, K., Braish, T., Eds.; CRC Press LLC: Boca Raton, FL, 2008; pp 217−229.
(48) While there is precedence for chromium-based methods for the oxidation of oxetan-3-ol, such methods necessitate the use of preparative GC for the separation of oxetan-3-one from byproducts, which we deemed to be impractical for the preparation of larger quantities: (a) Wojtowicz, J. A.; Polak, R. J. 3-Substituted oxetanes. *J. Org. Chem.* **1973**, *38* (11), 2061–6. (b) Kozikowski, A. P.; Fauq, A. H. Synthesis of novel 4-membered ring amino-acids as modulators of the N-methyl-D-aspartate (NMDA) receptor complex. *Synlett* **1991**, No. 11, 783–784.
(49) Stutz, W.; Waditschatka, R.; Winter, K.; Von Frieling, M.; Gressly, R.; Jau, B.; Buerki, S. Preparation of 3-Hydroxyoxetanes. EP 751136, 19960620, 1997.
(50) Details can be found in the following: Wuitschik, G. Oxetanes in Drug Discovery. Ph.D. Dissertation, ETH Zurich, Zurich, Switzerland, **2008**; DOI: 10.3929/ethz-a-005697432 (http://e-collection.ethbib.ethz.ch/view/eth:30903).
(51) Taber, D. F.; Amedio, J. C.; Jung, K. Y. Phosphorus pentoxide/dimethyl sulfoxide/triethylamine (PDT): a convenient procedure for oxidation of alcohols to ketones and aldehydes. *J. Org. Chem.* **1987**, *52* (25), 5621–5622.
(52) This compound has independently been reported by Jacobsen et al: Loy, R. N.; Jacobsen, E. N. Enantioselective intramolecular openings of oxetanes catalyzed by (salen)Co(III) xomplexes: access to enantioenriched tetrahydrofurans. *J. Am. Chem. Soc.* **2009**, *131* (8), 2786–2787.
(53) Chesney, A.; Marko, I. E. Synthetic approaches towards manzamine—an easy preparation of beta-amino aldehydes. *Synth. Commun.* **1990**, *20* (20), 3167–3180.
(54) For an example catalytic in rhodium, see the following: Fessard, T. C.; Andrews, S. P.; Motoyoshi, H.; Carreira, E. M. Enantioselective preparation of 1,1-diarylethanes: aldehydes as removable steering groups for asymmetric synthesis. *Angew. Chem., Int. Ed.* **2007**, *46* (48), 9331–9334.
(55) The Rh-catalyzed addition of boronic acids to Michael acceptors was pioneered by Hayashi and Miyaura. For key publications, see: the following: (a) Sakai, M.; Hayashi, H.; Miyaura, N. Rhodium-catalyzed conjugate addition of aryl- or 1-alkenylboronic acids to enones. *Organometallics* **1997**, *16* (20), 4229–4231. (b) Takaya, Y.; Ogasawara, M.; Hayashi, T.; Sakai, M.; Miyaura, N. Rhodium-catalyzed asymmetric 1,4-addition of aryl- and alkenylboronic acids to enones. *J. Am. Chem. Soc.* **1998**, *120* (22), 5579–5580. (c) Defieber, C.; Paquin, J.-F.; Serna, S.; Carreira, E. M. Chiral [2.2.2]dienes as ligands for Rh(I) in conjugate additions of boronic acids to a wide range of acceptors. *Org. Lett.* **2004**, *6* (21), 3873–3876. (d) Paquin, J.-F.; Defieber, C.; Stephenson, C. R. J.; Carreira, E. M. Asymmetric synthesis of 3,3-diarylpropanals with chiral diene−rhodium catalysts. *J. Am. Chem. Soc.* **2005**, *127* (31), 10850–10851.
(56) Alkylidene oxetanes may also be substrates for hydrazination/hydroazidation reactions: Waser, J.; Gaspar, B.; Nambu, H.; Carreira, E. M. Hydrazines and azides via the metal-catalyzed hydrohydrazination and hydroazidation of olefins. *J. Am. Chem. Soc.* **2006**, *128* (35), 11693–11712.
(57) A detailed description and validation of this method with classical "shake-flask" values have been described in the following: Fischer, H.; Kansy, M.; Wagner, B. Determination of High Lipophilicity Values. U.S. Pat. Appl. Publ. US 2006211121, 2006; F. Hoffmann-La Roche AG, Switzerland.